

Hierarchical Multidimensional Scaling for the Comparison of Musical Performance Styles

Anna K. Yanchenko and Peter D. Hoff
Department of Statistical Science
Duke University

December 22, 2024

Abstract

Quantification of stylistic differences between musical artists is of academic interest to the music community, and is also useful for other applications such as music information retrieval and recommendation systems. Information about stylistic differences can be obtained by comparing the performances of different artists across common musical pieces. In this article, we develop a statistical methodology for identifying and quantifying systematic stylistic differences among artists that are consistent across audio recordings of a common set of pieces, in terms of several musical features. Our focus is on a comparison of ten different orchestras, based on data from audio recordings of the nine Beethoven symphonies. As generative or fully parametric models of raw audio data can be highly complex, and more complex than necessary for our goal of identifying differences between orchestras, we propose to reduce the data from a set of audio recordings down to pairwise distances between orchestras, based on different musical characteristics of the recordings, such as tempo, dynamics, and timbre. For each of these characteristics, we obtain multiple pairwise distance matrices, one for each movement of each symphony. We develop a hierarchical multidimensional scaling (HMDS) model to identify and quantify systematic differences between orchestras in terms of these three musical characteristics, and interpret the results in the context of known qualitative information about the orchestras. This methodology is able to recover several expected systematic similarities between orchestras, as well as to identify some more novel results. For example, we find that modern recordings exhibit a high degree of similarity to each other, as compared to older recordings.

Keywords: audio processing, Bayes, hierarchical modeling, functional data, multidimensional scaling.

1 Introduction

The quantification of stylistic differences between musical artists is of interest in musicology, and has uses for the general music-listening public, such as for music information retrieval and recom-

mender systems. In this article, we are particularly focused on the quantification of systematic differences among ten different orchestras, based on data from audio recordings of the nine Beethoven symphonies. This is motivated by a desire to statistically quantify a variety of descriptions of heterogeneity among orchestras that has typically been done qualitatively, such as how musical performances might change over time, or how orchestras from the United States systematically differ from European orchestras.

In general, information about stylistic differences among artists can be obtained by comparing their performances of a common collection of musical pieces. Quantitative analyses of different orchestral recordings has been explored in the music information retrieval community using tempo curve analysis (Peperkamp et al., 2017) and image analysis techniques with principal components analysis (Liem and Hanjalic, 2015). A more statistical approach to making such comparisons would be to fit a model to the audio data for each artist separately, and then compare the estimated model parameters corresponding to each artist. However, from a data analysis perspective, an audio recording of a piece of music is a complex, multivariate, highly structured time series, with long-term dependencies that, in symphonic works, exist over multiple minutes. From a music information retrieval perspective, analysis of audio recordings has been of interest for areas such as calculating musical similarity for cover song identification (Raś and Wieczorkowska, 2010; Royo-Letelier et al., 2018) and recommendation systems (van den Oord et al., 2013), identifying and separating instruments (Vatolkin and Rudolph, 2018; Stoller et al., 2018) and aligning musical scores to audio recordings (Arzt and Lattner, 2018; Román et al., 2018). While the complexity of audio data allows for analysis of more nuanced features such as musical style, this complexity also makes it challenging to develop accurate generative statistical models of musical audio data in its raw form. One popular approach is to use convolutional neural networks with dilated, causal convolutions (van den Oord et al., 2016), and while these can generate audio that mimics their input, the large number of estimated parameters can be difficult to interpret, and potentially non-comparable across model fits. Additionally, WaveNet (van den Oord et al., 2016) models very short audio segments of only a few seconds in length, making stylistic analysis over full orchestral works that are multiple minutes in length challenging.

As an alternative to such generative approaches, for the purpose of identifying differences between orchestras, we propose to reduce the data from a set of audio recordings down to pairwise distances between orchestras, based on different musical characteristics of the recordings, such as tempo, volume dynamics, and timbre. For each of these characteristics, we obtain multiple pairwise distance matrices, one for each movement of each symphony, resulting in 37 distance matrices for each of the 3 musical characteristics. Comparison of the orchestras may then proceed using statistical methods appropriate for analysis of distance data. Such methods might include distance-based analysis of variance (ANOVA) approaches used in the ecological community (An-

derson, 2001; McArdle and Anderson, 2001; Minas and Montana, 2014; Rizzo and Szekely, 2010), or the related functional ANOVA (FANOVA) approach that was developed to analyze distance data in genomics with Gaussian processes (Vsevolozhskaya et al., 2014). In this article, we focus on adapting multidimensional scaling (MDS) to the specific task of combining information across multiple distance matrices in order to identify consistent differences between orchestras. MDS is a popular technique for analyzing distance data, originally developed in the psychology literature (Torgerson, 1952). Standard MDS generates an embedding of observed distance data into a Euclidean space so that the distances between objects in the embedding approximates the observed distances.

Our HMDS model can be viewed as a modification and extension of the Bayesian MDS model proposed by Oh and Raftery (2001). In Bayesian MDS (BMDS), the observed distance matrix is assumed to be equal to the distance matrix of a set of latent vectors in a Euclidean space, plus (truncated) Gaussian noise. Using a Markov chain Monte Carlo approximation algorithm, the posterior distribution of the latent vectors may be inferred from an observed matrix of distance data. Our proposed HMDS extends the BMDS model of Oh and Raftery (2001) in several ways in order to accommodate specific features of our data. Most importantly, BMDS was developed to analyze a single distance matrix, and assumes that the “true” distances are Euclidean. In contrast, our data consist of 37 distance values for each pair of orchestras and each musical characteristic. Treating these 37 values as “replicates” our HMDS model is able to distinguish between differences that are “systematic”, i.e. consistent across musical pieces, and differences that are idiosyncratic to particular pieces. Furthermore, our approach allows for the systematic component of the observed distance matrices to be non-Euclidean. This is useful, as the distance metrics we use to evaluate stylistic differences are not necessarily embeddable in Euclidean space. Another feature of our model is that we allow for differences in the potential for variation across replicates, or pieces. This is critical for our application, as some musical pieces have much more potential for variation than others. Combining information across pieces without adjusting for this potential would tend to hide systematic effects. Finally, in contrast to the truncated normal model in BMDS, we model non-negative distances using gamma distributions. This approach has the advantage of being able to accommodate skew in the distribution of observed distances, and is perhaps a more natural choice for positive distance data. Additionally, our gamma model for observed distances permits the use of semi-conjugate prior distributions, which facilitates several posterior calculations.

Related to our approach, Park et al. (2008) extended the BMDS model to multiple distance matrices in the specific context of capturing two types of heterogeneity in preference data. Their model combined two major types of latent utility models for preference data in a generalized, mixture model framework. However, in contrast to our work, Park et al. (2008) specified normally distributed likelihood functions for their observed dominance score matrices that were specific to the

two latent utility functions considered, as opposed to the general setting of skewed, positive distance data, as we consider here. Additionally, the model in Park et al. (2008) specified the same variance across the multiple distance matrices and assumed Euclidean distances between embedding vectors, while HMDS allows for heterogeneous potential for variation for each distance matrix and relaxes the Euclidean assumption. Additional extensions to BMDS include Bayesian MDS with variable selection (Lin and Fong, 2019), which incorporated covariate information in the dimensionality reduction performed by classical MDS and allowed for heterogeneous variability by distance pair, and Bayesian MDS with simultaneous variable selection with dimension reparameterization (Fong et al., 2015). In contrast to HMDS, though, both Lin and Fong (2019) and Fong et al. (2015) did not extend BMDS to multiple distance matrices and again assumed normal distributions for the observed distance data. In summary, our proposed HMDS model is distinguished from prior work such as Park et al. (2008); Lin and Fong (2019); Fong et al. (2015) by the extension to multiple distance matrices with heterogeneous variation, the modeling of non-negative distances with gamma distributions and the relaxation of the Euclidean assumption of the systematic component of our observed distance matrices.

The rest of this paper is organized as follows: the audio processing procedure and musical metrics are discussed in Section 2. In Section 3, we first review BMDS and then develop our HMDS model and provide an algorithm for posterior approximation. In Section 4 we fit an HMDS model to the audio recordings of all 9 Beethoven symphonies recorded by 10 different orchestras. We interpret the results and evaluate quantitatively the differences among the orchestras in the context of known, qualitative information. Our results recover several expected systematic similarities between orchestras, as well as identify some more novel results. For example, we find that modern recordings exhibit a high degree of similarity to each other, as compared to older recordings. Conclusions and directions for future work are discussed in Section 5.

2 Audio Feature Extraction

Fully parametric models of raw audio data can be highly complex, especially for our goal of identifying differences between orchestras. We thus propose to reduce the audio recordings for each piece to pairwise distances between orchestras, based on different musical characteristics of the recordings. Specifically, for each recording we create three positive functions of time, representing tempo, volume dynamics, and timbre over the duration of the recording. For each of these three audio characteristics and for each piece, a distance is computed between each pair of orchestras using the Hellinger metric distance between the corresponding functions. In the remainder of this section, we motivate this proposed audio processing methodology, starting with identification of musical features of interest, then the processing and aligning of the audio recordings and finally

comparison of the the audio features to form distance matrices. The audio processing details in this section are not required for an understanding of our proposed HMDS model and this section can be skipped.

2.1 Data and Features of Interest

Our original data consist of audio recordings of all nine Beethoven symphonies recorded by 10 different orchestras (Table 1) and the recordings span from the 1950s to 2016. Each movement is treated as a separate piece, resulting in a total of 37 pieces. For this work, we consider three main musical features of interest: tempo, dynamics and timbre. Overall, we are interested in extracting features that represent artistic or expressive choices made by conductors and orchestras, rather than features that are specific to the recording process. For example, the overall volume of a recording is a function of the microphone placement during the recording process, and is not an artistic choice made by the conductor. For all of the musical features considered, we attempt to isolate and remove artifacts of the recording process to focus on expressive musical features.

Table 1: Orchestras, conductors and recordings years for the audio recordings of the 9 Beethoven symphonies considered in this work.

Orchestra	Conductor	Recording Years
Academy of Ancient Music	Hogwood	1986-1989
Berlin Philharmonic	Rattle	2016
Berlin Philharmonic	von Karajan	1982-1984
Chicago Symphony Orchestra	Solti	1991
Leipzig Gewandhaus Orchestra	Masur	1989-1993
London Symphony Orchestra	Haitink	2006
NBC Symphony Orchestra	Toscanini	1939-1952
New York Philharmonic	Bernstein	1961-1967
Philadelphia Orchestra	Muti	1988-2000
Vienna Philharmonic	Rattle	2012

Tempo is the speed at which a piece is performed and often varies over the course of an orchestral piece of music. We are interested in relative tempo changes between orchestras and not in the overall speed of a recording. For example, if the score for a given piece calls for the tempo to accelerate at a specific point in the piece, one orchestra may accelerate over only one measure of music, while another orchestra may accelerate over three measures of music. Or, during the *accelerando* denoted in the musical score, one orchestra may double their tempo, while another orchestra may barely increase their speed at all. These types of relative tempo changes between orchestras are examples

of tempo features of interest.

Dynamics refer to the relative changes in volume of an orchestra over the course of a piece and we are interested in relative dynamic dissimilarities between orchestras, rather than the overall volume. For example, suppose the score for a given piece calls for a *crescendo*, or increase in volume, at a specific point in the piece. One orchestra may play twice as loud at the end of the crescendo as they did at the beginning of the crescendo, while another orchestra may not noticeably increase their volume at all over the crescendo.

Musical timbre refers to the quality or color of an orchestra’s sound. For example, a violin and a trombone have different timbres, and thus sound different from each other, even when playing the same note pitch. Individual orchestra members contribute to the overall differences in timbre between different orchestras and for this work, we consider the global timbre of the entire orchestra as a feature of interest. While several methods for analyzing timbre exist (Sueur, 2018; Grachten et al., 2013; Logan, 2000), we consider spectral flatness as a proxy for the timbre of the orchestra. Spectral flatness is a measure of the tonality of a sound, where a spectral flatness of 1 means that there are equal amounts of energy spread throughout the entire spectrum (white noise), while a spectral flatness close to 0 indicates that the energy in the audio signal is concentrated in only a few frequency bands, approaching a pure tone (Sueur et al., 2018).

Based on our measure of spectral flatness, a difference in timbre between two orchestras corresponds to a difference in the spread of energy across the spectrum. For example, at a specific point in a piece, the flutes in one orchestra may play as loud as the lower pitched instruments, resulting in a spread of energy across frequency bands and a high spectral flatness. On the other hand, an orchestra where only lower instruments play at a loud volume for the same part in the piece would have spectral energy concentrated in fewer frequency bands and thus a lower spectral flatness. Spectral flatness can be sensitive to the recording technology used to produce the audio signal. For example, older recordings that were converted from analog signals may have less energy in the upper frequencies, due to the audio conversion, and thus lower spectral flatness values compared to modern recordings that do not clip the upper frequencies. However, we believe that spectral flatness is a good initial proxy for the relative timbre features of an orchestra.

2.2 Audio Processing and Alignment

In this subsection, we describe the specific audio processing steps to transform the original audio recordings into data representations that can be used to calculate pairwise distances for each of the musical features or metrics of interest described above. Our procedure consists of three steps: spectral pre-processing, alignment and calculation of feature densities, each of which will be described in detail below.

2.2.1 Spectral Pre-Processing

Before calculating the musical metrics of interest, we need a musically meaningful representation of the audio signals that will allow for the calculation of these features. For example, we cannot determine the tempo of an orchestra for a given piece from the raw audio signal, so we will need another data representation that facilitates musical feature extraction. We use two different representations of the audio signal, the spectrogram and the chromagram. The spectrogram represents the power spectrum of the audio signal over the entire frequency range and is found via the Short-Time Fourier Transform (STFT). The spectrogram contains the energy distribution of the audio signal over time and is used to calculate the spectral flatness metric. The spectrogram for orchestra i for piece p is a $F \times T$ matrix, $S_{ip}(f, t)$, which represents the magnitude of the f^{th} frequency band at time t . For all orchestras and all pieces, the frequency resolution of the spectrogram representation is 5 Hz and the temporal resolution is 0.1 seconds. We only use the magnitude information from the spectrogram and ignore the phase information.

The chromagram representation (Müller, 2015) can be calculated from the spectrogram and is used to calculate the tempo and dynamics metrics. The chromagram aggregates the amplitude of each frequency bin in the spectrogram across octaves to give one amplitude for each pitch in the twelve tone scale. This aggregation is robust to differences in instrument balance and intonation between orchestras. The chromagram is a $12 \times T$ matrix, where each row corresponds to one note pitch. For orchestra i and piece p , let $\{f_q\}$ be the set of frequency bands that correspond to note pitch q . For example, $q = 11$ corresponds to a B^b note pitch, in any octave. Then, the chromagram, ψ_{ip} , can be calculated from the spectrogram as follows:

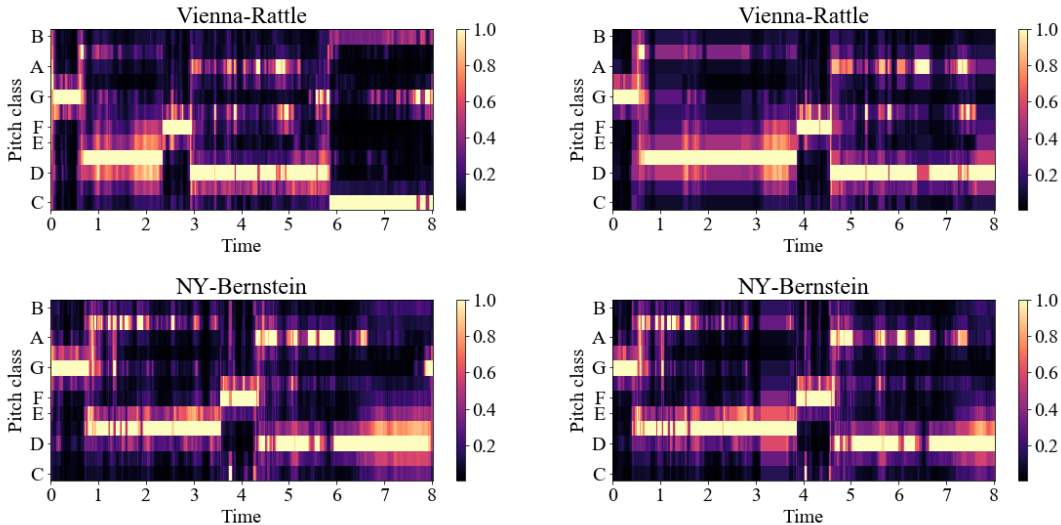
$$\psi_{ip}(q, t) = \sum_{k \in \{f_q\}} S_{ip}(k, t). \tag{1}$$

The 12-dimensional chromagram representation at time t , $\psi_{ip}(:, t)$, can be thought of as approximating the notes that orchestra i plays at time t . Example chromagrams are shown in Figure 1.

In summary, we calculate the spectrogram, S_{ip} , and chromagram, ψ_{ip} , representations for all orchestras i and pieces p . All of the musical features of interest are derived from these two representations; the tempo and dynamics features are calculated from the chromagram representation and the timbre features are calculated from the spectrogram representation.

2.2.2 Alignment

For all pieces p , orchestra i and orchestra j play the same notes in the same order. However, different orchestras may play these sequences of notes at different speeds. For example, in Figure 1a, the Vienna Philharmonic and the NY Philharmonic play the opening of Beethoven’s Fifth Symphony at different tempos; Vienna only holds the opening G pitch for about half a second



(a) Unaligned chromagrams.

(b) Aligned chromagrams.

Figure 1: (a) Unaligned and (b) aligned chromagrams for the opening of Beethoven No. 5 - Mvmt. 1 by the Vienna Philharmonic and the NY Philharmonic. The unaligned chromagrams show that the two orchestras play the same notes pitches, but at different speeds and for different durations, so these two orchestras do not perform the same part of the piece at the same point in time. However, after alignment, the two orchestras do perform the same part of the piece at the same point in time and musical features can be extracted.

and the following E^b pitch from 0.5 to 2.5 seconds, while NY plays the opening G for nearly an entire second and sustains the following E^b pitch for nearly three seconds. Our goal is to compare differences in tempo, dynamics and timbre when each orchestra is performing the *same part of each piece* to assess differences in artistic or expressive aspects of the performance. Before calculating the musical features of interest, we then need to temporally align the spectrogram and chromagram representations so that on piece p , at time t for orchestra i and at time t' for orchestra j , these two orchestras are performing the same part of the piece.

Since the chroma vectors approximate the notes that an orchestra plays at time t , we want to find the warping path of indices, $w(t)$, such that $\psi_{ip}(:, t) = \psi_{jp}(:, w(t))$ for all t , subject to the constraints that $w(t)$ is monotonically increasing and that the orchestras start and end at the same point in the piece, that is, $\psi_{ip}(:, 0) = \psi_{jp}(:, 0)$ and $\psi_{ip}(:, T_{ip}) = \psi_{jp}(:, T_{jp})$, where T_{ip} and T_{jp} are the lengths of piece p for orchestras i and j , respectively. This problem can be solved via dynamic time warping. Dynamic time warping finds a non-linear warping path, $w(t)$, between the two chromagrams and is frequently used in music information retrieval (Müller, 2015; Peperkamp et al., 2017; Thornburg et al., 2007; Ellis, 2007; Kirchhoff and Lerch, 2011; Kammerl et al., 2014).

Following Peperkamp et al. (2017), we align each piece to a reference MIDI recording from Kunstderfuge.com (2018) (MIDI is a symbolic music representation, and is simplified compared to the audio orchestral recordings). The result of the dynamic time warping is a warping path, $w_{ip}(t)$, for each orchestra i for each piece p , relative to the reference MIDI recording. Then, we have that $\psi_{ip}(:, w_{ip}(t)) \approx \psi_{jp}(:, w_{jp}(t))$ and $S_{ip}(:, w_{ip}(t)) \approx S_{jp}(:, w_{jp}(t))$ for all i, p and t . This equivalence is approximate, as specific chroma amplitudes can and do differ by orchestra; these differences correspond to variation in dynamics and timbre by orchestra, for example. After the alignment, however, all orchestras perform the same part of the piece at the same time. For simplicity, we also normalize the time by the length of each piece for each orchestra, so that $t \in [0, 1]$ for all orchestras i and pieces p . We can now use the aligned chromagrams and spectrograms to calculate our musical features of interest.

2.2.3 Calculation of Audio Feature Densities

After the alignment of our data representations, we are ready to calculate the specific musical metrics of interest. Starting with the aligned spectrograms and chromagrams, we calculate the tempo, dynamics and timbre features as a density that can be used to calculate pairwise distances between orchestras. Let $\tilde{\psi}_{ip}$ denote the aligned chromagrams, that is, $\tilde{\psi}_{ip}(:, t') = \psi_{ip}(:, w(t))$, and similarly for the aligned spectrograms, \tilde{S}_{ip} , that will be used for the calculation of these musical metric densities. Example densities are shown in Figure 2.

The tempo density curve can be calculated using the warping path from the dynamic time warping alignment. That is, the tempo density for orchestra i on piece p is

$$\mu_{ip}(t) \propto w'_{ip}(t) = \frac{dw_{ip}(t)}{dt},$$

where $\mu_{ip}(t)$ is the ratio of the tempo of orchestra i on piece p at time t relative to the reference recording for piece p . This means that at time t for piece p , if $\mu_{ip}(t) = 4$ and $\mu_{jp}(t) = 2$, then orchestra i is playing two times as fast as orchestra j . Likewise, $\mu_{ip}(t) < 1$ means that orchestra i is performing piece p slower than the reference recording at time t . The tempo curve is normalized such that

$$\mu_{ip}(t) = \frac{w'_{ip}(t)}{\sum_{s=0}^1 w'_{ip}(s)}.$$

The dynamics density curve can be calculated using the sum of the magnitudes of the aligned chromagram at each point in time, divided by the average volume for the entire piece. That is, the dynamics are calculated as

$$v_{ip}(t) \propto \frac{\sum_{q=1}^{12} \tilde{\psi}_{ip}(q, t)}{\frac{1}{12} \sum_{q=1}^{12} \sum_{s=0}^1 \tilde{\psi}_{ip}(q, s)}.$$

We normalize the dynamics curves by the average volume for that orchestra for piece p , as we are not interested in the overall volume of each orchestra. Again, we define $v_{ip}(t)$ to be a density,

so that $\sum_{s=0}^1 v_{ip}(s) = 1$. Then, $v_{ip}(t) > v_{jp}(t)$ means that relative to each orchestra’s respective average dynamic for piece p , orchestra i is playing louder than orchestra j at time t .

Spectral flatness is the ratio of the geometric mean to the arithmetic mean and can be calculated as

$$\phi_{ip}(t) \propto F \times \frac{\sqrt[F]{\prod_{f=1}^F \tilde{S}_{ip}(f, t)}}{\sum_{f=1}^F \tilde{S}_{ip}(f, t)},$$

where $\tilde{S}_{ip}(f, t)$ is the relative amplitude of the f^{th} frequency of the aligned spectrogram and F is the total number of frequencies for the aligned spectrogram (Sueur et al., 2018) and we have that $\sum_{s=0}^1 \phi_{ip}(s) = 1$. For the spectral flatness features, $\phi_{ip}(t) > \phi_{jp}(t)$ means that the energy of orchestra j is concentrated in a smaller number of frequency bands than orchestra i for piece p at time t .

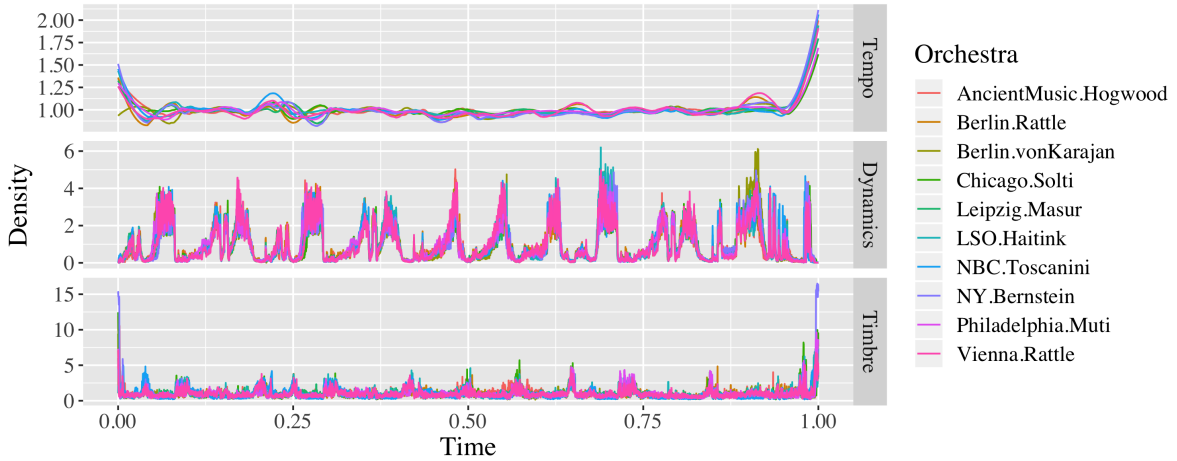


Figure 2: Tempo, dynamics and timbre/spectral flatness densities for all 10 orchestras for Beethoven Symphony No. 6, Movement 1. The time is also normalized to be between 0 and 1, since all recordings are already aligned to the same reference recording.

In summary, after transforming the audio signals to spectrogram and chromagram representations, temporally aligning the representations and calculating the musical metrics for tempo, dynamics and timbre, we have musical feature densities for tempo, $\mu_{ip}(t)$, dynamics, $v_{ip}(t)$ and timbre, $\phi_{ip}(t)$, for all orchestras $i = 1, \dots, 10$, pieces $p = 1, \dots, 37$ and time $t \in [0, 1]$. These curves are densities and normalized to sum to 1, such that $\sum_{s=0}^1 \mu_{ip}(s) = \sum_{s=0}^1 v_{ip}(s) = \sum_{s=0}^1 \phi_{ip}(s) = 1$.

2.3 Comparison of Audio Features

Now that we have densities for each orchestra, for each piece and for each musical feature, we can calculate pairwise distance matrices using a density-based distance measure. We calculate the

pairwise Hellinger distance between all orchestras for each piece to obtain 3-dimensional distance arrays for each musical metric. The Hellinger distance is a commonly used density-based distance measure and for discrete distributions $P = (p_1, \dots, p_K)$ and $Q = (q_1, \dots, q_K)$ can be calculated as

$$H(P, Q) = \frac{1}{\sqrt{2}} \sqrt{\sum_{i=1}^K (\sqrt{p_i} - \sqrt{q_i})^2}. \quad (2)$$

After calculating the pairwise Hellinger distance between orchestras, the distances within each metric are normalized to be between 0 and 1 over all pieces. The end result of the audio feature extraction procedure is an $N \times N \times M$ distance array for each of the three musical metrics, tempo, D^μ , dynamics, D^ν , and timbre, D^ϕ , where $N = 10$ is the number of orchestras and $M = 37$ is the number of pieces. Then, for a specific musical metric, y_{ijp} is the corresponding entry in the $N \times N \times M$ metric array, representing the distance between orchestra i and orchestra j on piece p for that musical metric. We treat these y_{ijp} distances as our observed data for the modeling described in the next section.

The overall audio processing methodology can thus be summarized as follows. We start with audio recordings of all nine Beethoven symphonies by N different orchestras. Each movement of a symphony is treated as a separate piece, resulting in M pieces. Using spectrogram and chromagram representations of the audio signals, we temporally align the orchestra representations by piece using dynamic time warping, and calculate tempo, dynamics and timbre densities by piece. Then, we use the Hellinger density-based distance measure to calculate $N \times N \times M$ pairwise replicate distance matrices for each of the three musical metrics. The data and accompanying code is released at <https://github.com/aky4wn/HMDS>.

3 Hierarchical Multidimensional Scaling

In this section, we develop Hierarchical Multidimensional Scaling, a statistical model for a sample of pairwise distance matrices among a common set of objects. The purpose of the model is to identify patterns in the distance matrices that are consistent throughout the sample as well as to quantify the variation of the distance matrices around these patterns. For example, in our application, each matrix in our sample represents the pairwise distance between two orchestras for a given piece for a specific musical metric, either tempo, dynamics or timbre. Our model-based approach is a modification and extension of the approach of Oh and Raftery (2001), who developed a probability model for a single dissimilarity matrix.

3.1 Bayesian Multidimensional Scaling

Oh and Raftery (2001) propose Bayesian Multidimensional Scaling (BMDS), a model-based version of classical MDS. For a *single* data matrix of pairwise distances between objects, the goals of BMDS are to find a low-dimensional representation of the objects of interest in Euclidean space and to measure the discrepancy between the Euclidean space and the observed distances. BMDS assumes that observed pairwise distance measurements are equal to a true distance measure plus observational noise, where the true distance measure is the Euclidean distance between latent embedding vectors for the pair. Let N be the number of objects or entities of interest and y_{ij} be the observed distance between object i and object j . Then, the BMDS model is defined as follows:

$$y_{ij} \sim \text{TruncNorm}(\|X_i - X_j\|_2, \sigma^2), \quad j > i, \quad i, j = 1, \dots, N, \quad (3)$$

independently, where X_1, \dots, X_N are unobserved latent vectors in r -dimensional Euclidean space, one for each object i , and σ^2 is an unknown scale parameter. TruncNorm is the normal density, truncated to be above 0. Note that for BMDS, the error term σ^2 represents the deviation of the observed distances from Euclidean distances, which could be attributed to either measurement error or misspecification of the (true) distances being Euclidean.

Oh and Raftery (2001) describe a Markov Chain Monte Carlo algorithm for approximating the posterior distribution of X_1, \dots, X_N and σ^2 , conditional on the observed distance data $\{y_{ij} : j > i\}$. They specify independent priors for each of the unknown parameters. The latent X_i vector for each object is assumed to come from an independent, r -dimensional normal distribution with diagonal covariance matrix Λ , where the diagonal elements of Λ are inverse-gamma distributed. The error term, σ^2 , is assigned an inverse-gamma prior distribution for conjugacy. The original BMDS model does not consider replications or multiple distance matrices, though later extensions do for a specific preference data application (Park et al., 2008), as discussed in Section 1.

3.2 Hierarchical MDS for Multiple Distance Matrices

Given only a single distance matrix of observed distances, the BMDS model cannot distinguish between measurement error and the degree to which the systematic distances between objects differ from being Euclidean. For example, a large estimated σ^2 value in Equation 3 could indicate a large amount of measurement error in the observed pairwise distances *or* that the observed distances are not well represented by Euclidean distances between latent vectors (or some combination of these two factors). With *replicate distance matrices*, however, there is sufficient information to distinguish a non-Euclidean mean distance from across-sample measurement variation. We quantify the variation of the replicate distance matrices around a common mean distance matrix with the following hierarchical MDS (HMDS) model. Let y_{ijp} be the observed pairwise distance between

entity i and entity j for observation p , where there are N total entities and M total replicate distance matrices. The HMDS model is given in Equation 4:

$$y_{ijp} \sim \text{Gamma} \left(\psi, \frac{\psi}{\tau_p \delta_{ij}} \right), \quad j > i, \quad i, j = 1, \dots, N, \quad p = 1, \dots, M, \quad (4)$$

independently across pairs and replicates, where $\psi, \tau_1, \dots, \tau_M$ and $\{\delta_{ij} : j > i\}$ are parameters to be estimated. The gamma distribution is parameterized such that the mean of y_{ijp} is $\tau_p \delta_{ij}$ and the variance of y_{ijp} is $(\tau_p^2 \delta_{ij}^2) / \psi$. Each τ_p is a scale parameter for replicate distance matrix p that allows for each matrix to have a different “potential” for variation. The $\{\delta_{ij} : j > i\}$ parameters represent the systematic dissimilarity between entities i and j across all M replicate matrices, while the ψ parameter serves as an overall scale factor.

Inclusion of the τ_1, \dots, τ_M parameters is important in our application, as we expect some pieces to have more inherent opportunities for variation than other pieces. For example, some pieces have numerous vague tempo markings that allow for a good deal of artistic interpretation and tempo variation between orchestras, as compared to other pieces that do not have many denoted changes in tempo. However, a piece’s “potential” for variation is a characteristic of the piece and is separate from the systematic differences between orchestras, and must be handled accordingly. This potential for variation scales both the mean and the variance of the observed distances.

The proposed HMDS model differs in several ways from the BMDS model. First, the gamma distribution for the observed pairwise distances is a more natural choice for a positive random quantity than the truncated normal distribution of BMDS. The gamma distribution allows for skew in the observed pairwise dissimilarities and facilitates straightforward parameter estimation and inference, as will be described below. Second, the HMDS model in Equation 4 does not restrict the $\{\delta_{ij} : j > i\}$ parameters to correspond to Euclidean distances. This relaxes the assumptions of BMDS and is important in many applications, including our comparison of orchestral recordings, where the distance metrics used to compare objects are known to be non-Euclidean.

The HMDS parameters can be estimated with maximum likelihood estimation. The MLE estimates for the δ_{ij} and τ_p parameters satisfy the following system of equations:

$$\hat{\delta}_{ij}^{MLE} = \frac{1}{M} \sum_{p=1}^M \frac{y_{ijp}}{\hat{\tau}_p^{MLE}}, \quad \hat{\tau}_p^{MLE} = \frac{2}{N(N-1)} \sum_{i=1}^N \sum_{j>i} \frac{y_{ijp}}{\hat{\delta}_{ij}^{MLE}}.$$

The MLE for ψ can be found by iteratively solving the following equation:

$$\frac{\Gamma'(\psi)}{\Gamma(\psi)} - \log \psi = \frac{2}{N(N-1)M} \left[1 + \sum_{i=1}^N \sum_{j>i} \sum_{p=1}^M \left(\log \left(\frac{y_{ijp}}{\tau_p \delta_{ij}} \right) - \frac{y_{ijp}}{\tau_p \delta_{ij}} \right) \right],$$

where $\Gamma'(\psi)$ is the digamma function, $\Gamma'(\psi) = \frac{d\Gamma(\psi)}{d\psi}$. Importantly, note that the MLE estimates, $\hat{\delta}_{ij}^{MLE}$, might not be distances.

We choose to perform Bayesian inference for parameter estimation. Bayesian inference in the HMDS model naturally allows for parameter uncertainty estimates. Additionally, the space of $N \times N$ distance matrices is quite high-dimensional and complex, and Bayesian inference provides shrinkage towards a lower dimensional space. Finally, the choice of a hierarchical model for the $\{\delta_{ij} : j > i\}$ parameters centered around a Euclidean space can aid in parameter interpretation. That is, we can specify a prior that puts the $\{\delta_{ij} : j > i\}$ parameters near some actual distances that satisfy the triangle inequality. To that end, we model the $\{\delta_{ij} : j > i\}$ parameters as

$$\delta_{ij} \sim \text{Inv-Gamma}(\gamma, (\gamma + 1)\|X_i - X_j\|_2), \quad j > i, \quad i, j = 1, \dots, N, \quad (5)$$

independently across pairs. The inverse-gamma distribution is parameterized such that the prior mode for δ_{ij} is $\|X_i - X_j\|_2$. The goal of the prior is to shrink the dissimilarity between orchestras i and j towards a distance metric that follows the triangle inequality. The $\|X_i - X_j\|_2$ term fixes this metric space as an $N - 1$ dimensional Euclidean space, though the γ parameter allows for potentially substantial variation from this Euclidean distance. Notably, this variation about a Euclidean distance, represented by the γ parameter in HMDS, is separate from the across-replicate sampling variability, represented by the parameter ψ . This separation of sources of variation is in contrast to the BMDS model.

This particular choice of an inverse-gamma prior further facilitates computation and interpretation. The effect of the prior on estimation of the δ_{ij} 's can be understood from the form of their full conditional distributions. The conditional density of δ_{ij} given all other model parameters and the observed y_{ijp} pairwise distances is

$$\delta_{ij} \Big| \psi, \gamma, \tau_1, \dots, \tau_M, X_1, \dots, X_N, Y \sim \text{Inv-Gamma} \left(M\psi + \gamma, (\gamma + 1)\|X_i - X_j\|_2 + \psi \sum_{p=1}^M \frac{y_{ijp}}{\tau_p} \right),$$

where $Y = \{y_{ijp} : i = 1, \dots, N, j > i, p = 1, \dots, M\}$. The mode of this conditional distribution is

$$\frac{\gamma + 1}{M\psi + \gamma + 1} \|X_i - X_j\|_2 + \frac{M\psi}{M\psi + \gamma + 1} \hat{\delta}_{ij}^{MLE},$$

so the δ_{ij} prior specified in Equation 5 shrinks the MLE estimate towards a set of Euclidean distances.

The full conditional distribution of the τ_p parameters, given all other model parameters and the observed y_{ijp} pairwise distances is

$$\tau_p \Big| \psi, \gamma, \{\delta_{ij} : j > i\}, X_1, \dots, X_N, Y \sim \text{Inv-Gamma} \left(\frac{N(N-1)}{2} \psi + 1, \psi \sum_{i=1}^N \sum_{j>i} \frac{y_{ijp}}{\delta_{ij}} \right),$$

and the conditional mode is

$$\frac{\psi N(N-1)}{\psi N(N-1) + 4} \hat{\tau}_p^{MLE}.$$

The conditional mode of τ_p depends on how close the observed pairwise distances (the y_{ijp} 's) are to the systematic dissimilarities (the δ_{ij} 's) across all pairs, $j > i$. That is, if $y_{ijp} = \delta_{ij} \forall j > i, i = 1, \dots, N$, then $\hat{\tau}_p^{MLE} = 1$ and the variation of the y_{ijp} distances is only scaled by ψ . In this case, the observed distances are equal to the systematic dissimilarities and there is no ‘‘potential’’ for variation for replication matrix p . However, when $y_{ijp} > \delta_{ij}$ across object pairs for a given replication matrix p , then $\hat{\tau}_p^{MLE} > 1$ and that specific replication p has a high ‘‘potential’’ for variation.

For a full Bayesian analysis, we also need to specify priors for the remaining unknown parameters:

$$\begin{aligned} X_1, \dots, X_N &\overset{indep.}{\sim} N_r(0, \Lambda) \\ \psi &\sim \text{Gamma}(a_1, b_1) \\ \gamma &\sim \text{Gamma}(a_2, b_2) \\ \tau_1, \dots, \tau_M &\overset{indep.}{\sim} \text{Inverse-Gamma}(\alpha, \beta) \end{aligned} \tag{6}$$

where Λ is a diagonal matrix and $a_1, b_1, a_2, b_2, \alpha$ and β are positive scalars. We set $a_1, b_1, a_2, b_2, \alpha$ and β to 0.01 in our application. We also use an empirical Bayes approach to setting Λ by estimating the variance of embedding vectors from classical MDS performed for each piece.

The joint posterior distribution of model parameters can be approximated with a Markov Chain Monte Carlo algorithm. One such algorithm proceeds as follows:

1. For each $i = 1, \dots, N, j > i$, simulate

$$\delta_{ij} \sim \text{Inv-Gamma} \left(M\psi + \gamma, (\gamma + 1)\|X_i - X_j\|_2 + \psi \sum_{p=1}^M \frac{y_{ijp}}{\tau_p} \right).$$

2. For each $p = 1, \dots, M$, simulate

$$\tau_p \sim \text{Inv-Gamma} \left(\alpha + \frac{N(N-1)}{2}\psi, \beta + \psi \sum_{i=1}^N \sum_{j>i} \frac{y_{ijp}}{\delta_{ij}} \right).$$

3. The remaining parameters, $\{X_1, \dots, X_N, \psi, \gamma\}$, can be updated via Metropolis-Hastings steps.

Full details of the Markov Chain Monte Carlo algorithm are given in Appendix A.

4 Analysis of Orchestral Distance Data

In this section, we fit the HMDS model to the replicate orchestral distance matrices to explore systematic differences between orchestras across pieces. We fit the HMDS model separately for

each of the three musical distance metrics: tempo, dynamics and timbre. We check the MCMC approximation outlined in Section 3.2 and examine the goodness-of-fit of HMDS for our orchestral audio data. Finally, we analyze the learned parameters for each musical metric and find that the HMDS model is able to recover musically expected systematic differences between orchestras across pieces, as well as suggest some unexpected similarities between orchestras.

4.1 MCMC Approximation and Goodness-of-Fit

The posterior distribution of parameters in the HMDS model can be approximated using a Markov Chain Monte Carlo (MCMC) algorithm, such as the one described in Section 3.2 or a more general MCMC algorithm (Stan Development Team, 2019). We fit the HMDS model in Rstan with the default No-U-Turn Hamiltonian Monte Carlo sampler. Parameter values were randomly initialized and the chain was run for 30000 iterations, where the first 15000 iterations were discarded as burn-in and no thinning was performed. The final 15000 iterations were retained for posterior inference. We diagnose the posterior approximation with trace plots and effective sample size (ESS) diagnostics (Stan Development Team, 2019).

Trace plots for a subset of the τ_p parameters for the tempo metric are shown in Figure 3 and trace plots for the remaining metrics are included in Appendix B. All trace plots appear stationary for the 15000 posterior simulations used for analysis. The median ESS values across all M pieces for the τ_p parameters are 407 for the tempo metric, 189 for the dynamics metric and 274 for the timbre metric. While the ESS values for the τ_p parameters do indicate that the posterior Markov chains are mixing slowly, the trace plots across parameters and musical metrics appear stationary.

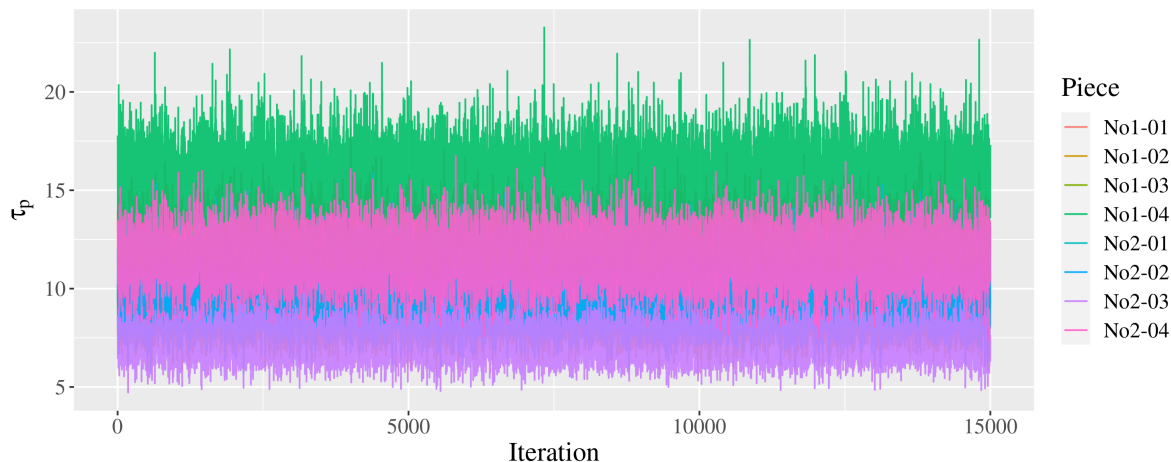


Figure 3: Trace plot for Symphonies No. 1 and No. 2 (corresponding to $p = 1, \dots, 8$) for τ_p for the tempo metric.

We also analyze the goodness-of-fit of the HMDS model for our orchestral audio data using posterior predictive checks (Gelman et al., 2014). We can evaluate the goodness of fit of the pair-specific sampling model by simulating posterior predictive values, $\tilde{y}_{ijp} \sim \text{Gamma}(\psi, \psi/(\tau_p \delta_{ij}))$, at each iteration of the Markov chain. These values can be compared to the observed y_{ijp} 's to evaluate the fit of the pair-specific sampling model by computing $r_{ijp} = \tilde{y}_{ijp}/y_{ijp}$ for each simulated \tilde{y}_{ijp} , where the ratio accounts for differences in scale due to τ_p . The distribution of these ratios for one orchestra pair and all pieces for the tempo metric is displayed in Figure 4. Additionally, we can evaluate the coverage of these difference distributions. For the tempo metric, 95.14% of the 95% highest-posterior density (HPD) intervals for each r_{ijp} contain 1. Likewise, 95.79% and 95.38% of the 95% HPD intervals for r_{ijp} contain 1, for dynamics and timbre, respectively. Overall, these results indicate that the sampling model for HMDS fits the data well.

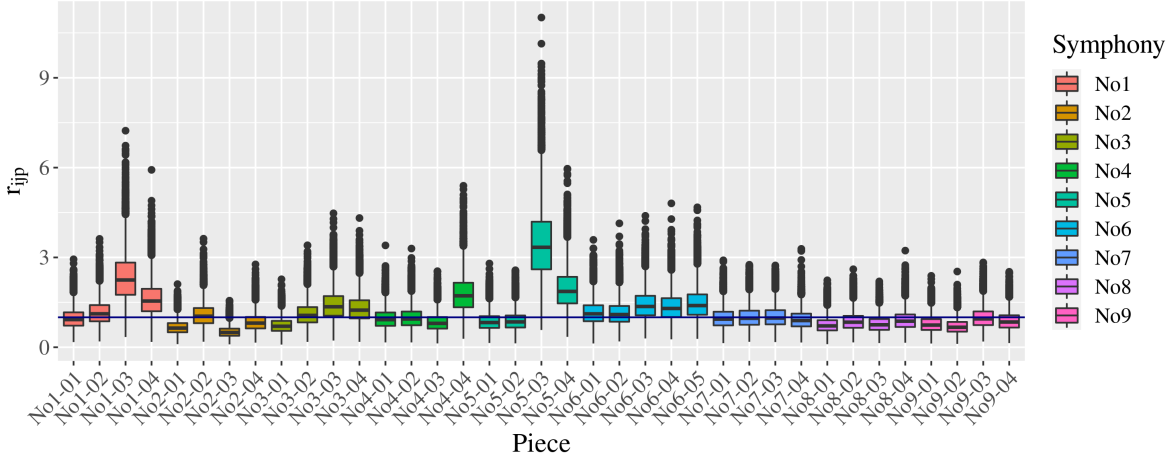


Figure 4: Posterior predictive checks for the HMDS sampling model for one orchestra pair (Academy of Ancient Music and Vienna-Rattle) across all pieces for the tempo metric, $r_{ijp} = \tilde{y}_{ijp}/y_{ijp}$.

Likewise, we can evaluate the goodness-of-fit of the hierarchical portion of HMDS with posterior predictive checks. At each iteration of the Markov chain, we can calculate $\|X_i - X_j\|_2$, simulate $\tilde{\delta}_{ij} \sim \text{Inv-Gamma}(\gamma, (\gamma + 1)\|X_i - X_j\|_2)$ and then simulate posterior predictive values, $\tilde{y}_{ijp} \sim \text{Gamma}(\psi, \psi/(\tau_p \tilde{\delta}_{ij}))$. We compute $e_{ijp} = \tilde{y}_{ijp} - y_{ijp}$ for each simulated \tilde{y}_{ijp} and the distribution of these differences for all orchestra pairs, averaged across pieces (i.e. \bar{e}_{ij}) is displayed in Figure 5. Again, we can access the coverage of the distribution of \bar{e}_{ij} ; 97.96%, 100% and 99.64% of the 95% HPD intervals for \bar{e}_{ij} for the tempo, dynamics and timbre metrics, respectively, contain 0.

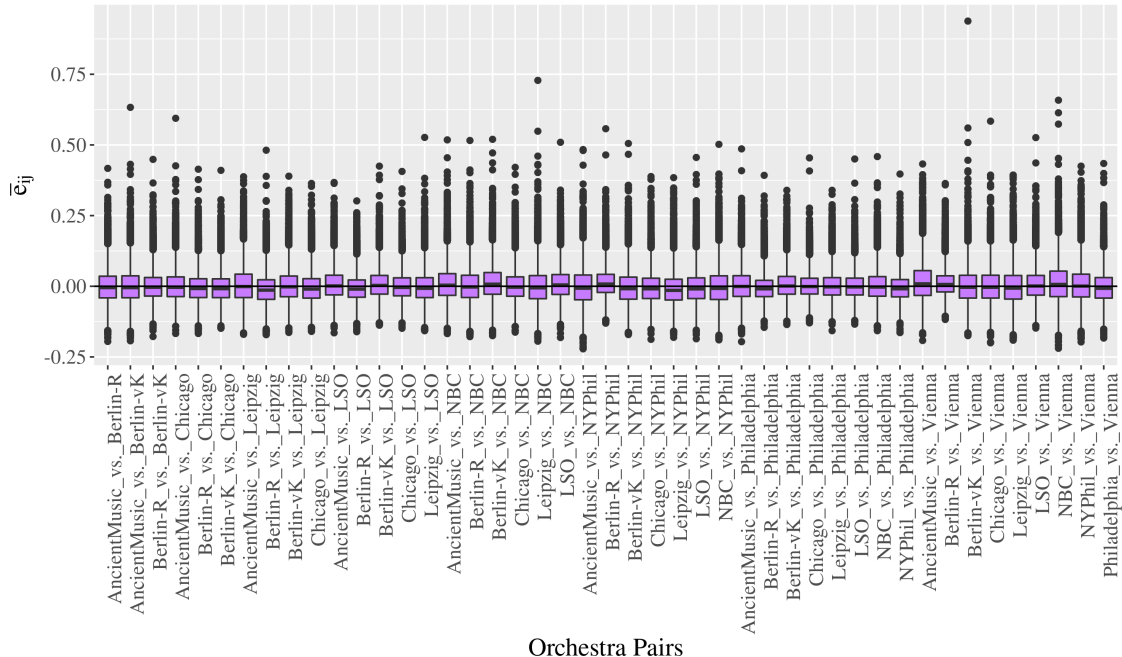


Figure 5: Posterior predictive checks for the hierarchical sampling model for the tempo metric, averaged across all pieces.

4.2 Potential for Variation by Piece

The τ_p parameters were introduced into the HMDS model to account for heterogeneous variation in the potential for across-orchestra differences by piece, where this potential for variation is determined by musical characteristics of the specific piece. The posterior distributions for each piece for τ_p are given in Figure 6 for the tempo metric, and in Appendix B for dynamics (Figure 15) and timbre (Figure 16). Across all three metrics, the τ_p parameters were able to recover the different potentials for across-orchestra variation by piece, and the results correspond to musical expectation based on the score of each piece.

For example, for the tempo metric, the posterior mean of τ_p for Symphony No. 6, Movement 1 (No6-01) was among the lowest for all pieces, while Symphony No. 9, Movement 2 (No9-02) was the highest posterior mean (Figure 6). This suggests that there is more potential for across-orchestra variation in tempo for No9-02 than for No6-01. Indeed, this corresponds to features of the musical score for these two pieces (International Music Score Library Project, 2019): piece No9-02 has approximately 24 marked tempo changes, while piece No6-01 has no marked tempo changes and only a fermata on the last note of the piece. (We include fermatas and grand pauses in our approximate count of marked tempo changes. A fermata indicates that a note should be held for a length of time determined by the conductor, while a grand pause indicates a break of complete

silence in the piece for an amount of time again determined by the conductor). Each tempo change denoted in the score is relative, thus allowing for a high level of variation in interpretation between different orchestras on pieces with many marked tempo changes. While tempo changes that are not written in the score can and do occur, the score is the “ground truth” and a proxy for the expected potential of variation. The posterior distributions of the τ_p parameters for the dynamics and timbre metrics are summarized in Appendix B and also show a correspondence to musical markings in the score of each piece.

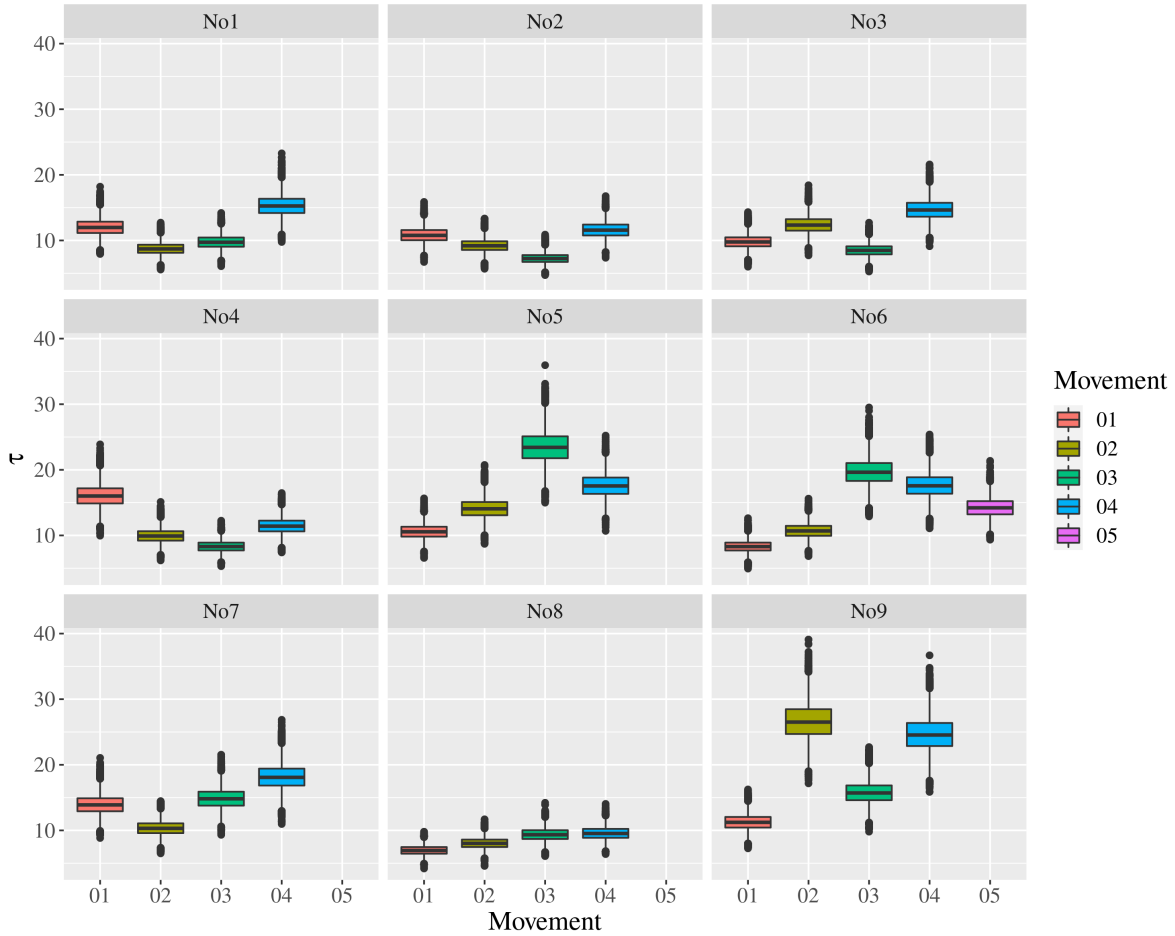


Figure 6: Posterior distributions for the τ_p parameters for the tempo metric, by Beethoven symphony. The τ_p parameters were able to recover the variation in the potential for across-orchestra differences by piece, for example, No9-02 as compared to No6-01.

4.3 Systematic Differences Between Orchestras

The primary motivation for this work was to explore systematic variation between orchestras across pieces for various musical metrics, with the secondary goal of relating systematic differences to known characteristics of the orchestra and recording, such as the year of the recording. The latent distance parameters $\{\delta_{ij} : j > i\}$ in the HMDS model capture this systematic variation and are the main parameters of interest for our application. From a musical perspective, we do expect systematic differences between orchestras. For example, the Academy of Ancient Music performs on period instruments, which sound different (in terms of dynamics and timbre) from the modern instruments used by the other orchestras considered here. Additionally, the musical metrics that we consider can be strongly influenced by the conductor, so we expect the two orchestras under Sir Simon Rattle (Berlin and Vienna) to be similar. As we will show, the HMDS model is able to recover these expected musical results and to additionally suggest some orchestral similarities that are more surprising.

For each metric, we present a summary of the δ_{ij} 's as a heatmap and a dendrogram formed via hierarchical agglomerative clustering. For each heatmap, darker colors correspond to smaller values of δ_{ij} , which indicate that orchestra i and orchestra j are more similar to each other. For each dendrogram, orchestras that are more similar to each other are joined together at a lower height on the dendrogram. We focus on the posterior mean of each δ_{ij} , as the posterior distribution of each δ_{ij} is not skewed and fairly symmetric (Figure 17). Additionally, at each iteration of the Markov chain, the δ_{ij} values are very close to the values $\|X_i - X_j\|_2$ and thus satisfy the triangle inequality.

4.3.1 Tempo

A heatmap and dendrogram representing the estimated δ_{ij} 's for the tempo metric are provided in Figure 7a and Figure 7b, respectively. As expected, the recordings by Sir Simon Rattle with the Vienna Philharmonic and the Berlin Philharmonic are quite similar across pieces. These recordings were made within 5 years of each other under the same conductor, and the conductor has a large degree of control over the tempo of each piece. Additionally, the two Rattle recordings are also very similar to the LSO-Haitink recordings in terms of tempo. The data from these three orchestras are the most recent, in terms of the year in which the recordings were made. However, there does not appear to be any clear evidence of consistent similarity between orchestras by continent. Somewhat surprisingly, the Academy of Ancient Music and the NBC Symphony Orchestra are similar to each other, and quite different from the other orchestras. This result can be interpreted in terms of the style of both orchestras and the scholarship of their conductors. The Academy of Ancient Music uses scholarship to imitate the way that these pieces would have been performed in Beethoven's time. The NBC Symphony Orchestra recordings, on the other hand, were conducted by Arturo Toscanini (born in 1867), who was a contemporary of musicians that were alive in Beethoven's time

(Beethoven died in 1827) and who studied a style of conducting similar to that of the era when these pieces were composed.

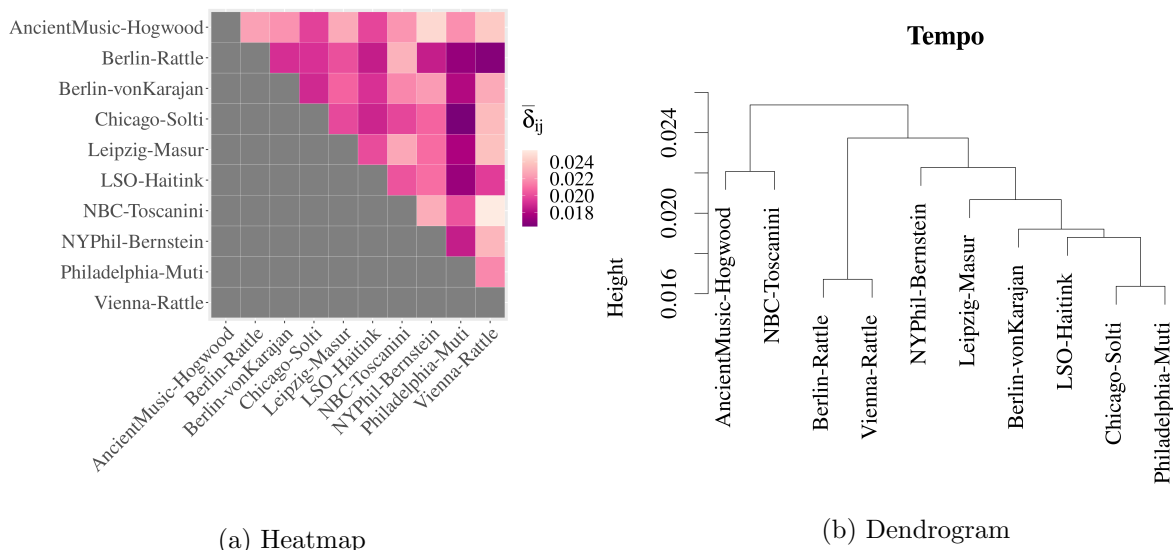


Figure 7: (a) Heatmap of the posterior means of δ_{ij} and (b) dendrogram found via hierarchical agglomerative clustering on the posterior mean of δ_{ij} for the tempo metric. The two recordings by Rattle with Vienna and Berlin are very similar.

4.3.2 Dynamics

The estimates of the δ_{ij} 's for the dynamics metric also confirm prior musical expectations. In both the heatmap (Figure 8a) and the dendrogram (Figure 8b) for dynamics, the Academy of Ancient Music appears to be an outlier. This is expected, as Ancient Music is the only orchestra to record on period instruments, which cannot play as loudly as modern instruments. Thus, the contrast in the range of dynamics (from loudest to softest volume) is smaller on period instruments than modern orchestral instruments. NBC also performed on older instruments (from the 1950s), which were not as loud as the modern orchestral instruments used by the remaining orchestras. Unlike the tempo metric, the dynamics metric shows evidence for some clustering by continent (Figure 8b). Vienna-Rattle, Berlin-von Karajan and LSO-Haitink are very similar, while all of the American orchestras are on the same main branch of the dendrogram. Finally, as shown in Figure 8a, there is again evidence for higher similarity between more modern recordings, as Vienna-Rattle, Berlin-Rattle, LSO-Haitink and Philadelphia-Muti are very similar.

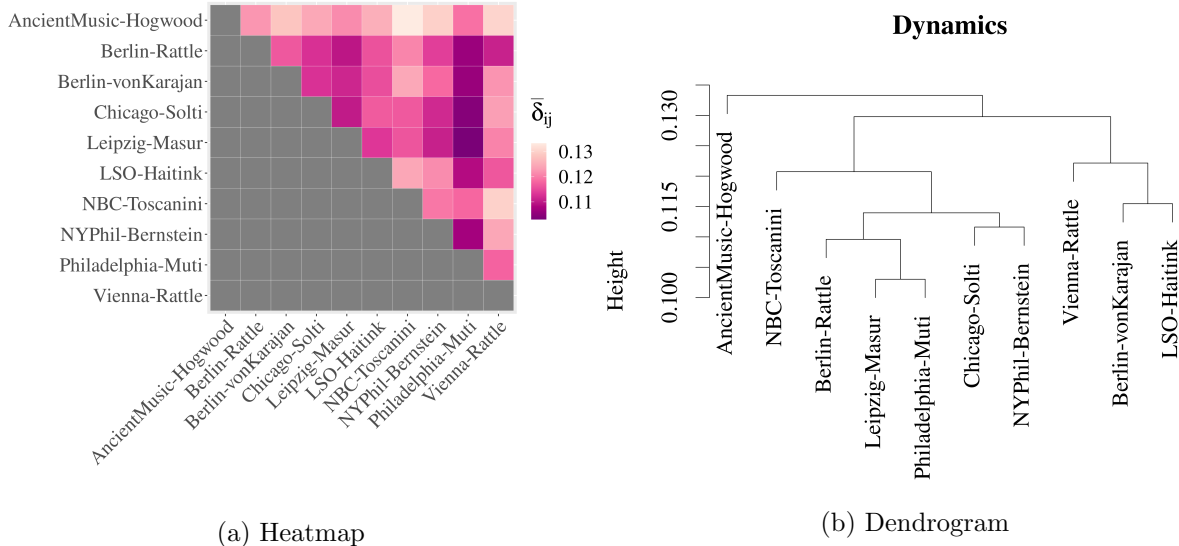


Figure 8: (a) Heatmap of the posterior means of δ_{ij} and (b) dendrogram found via hierarchical agglomerative clustering on the posterior mean of δ_{ij} for the dynamics metric. The Academy of Ancient Music appears to be an outlier.

4.3.3 Timbre/Spectral Flatness

Finally, the analysis of the posterior means of δ_{ij} for timbre again align with our musical expectation. Ancient Music is again an outlier for the timbre metric, due to the use of period instruments which have a fundamentally different timbre than modern orchestral instruments (Figure 9a). Additionally, the NBC-Toscanini recordings and NY-Bernstein recordings are similar to each other and different from most of the other orchestras (Figure 9b), likely due to specifics of the recording technology at the time these recordings were made. Again, there is evidence for newer recordings being more similar to each other, as the LSO-Haitink, Berlin-Rattle, Chicago-Solti and Philadelphia-Muti are quite similar to each other in Figure 9b. Finally, there is no consistent evidence for similarity by continent. While the NY-Bernstein recordings are similar to Chicago and Philadelphia in Figure 9a, Philadelphia is also very similar to several European orchestras.

5 Conclusions and Future Work

In order to quantify systematic differences between orchestras, we developed a hierarchical, model-based approach to multidimensional scaling. This method generalized the BMDS model of Oh and Raftery (2001) in several ways, including the extension to modeling heterogeneous replicate distance matrices. We applied HMDS to the comparison of different orchestras across the Beethoven symphonies. The proposed HMDS model was successful in uncovering systematic differences be-

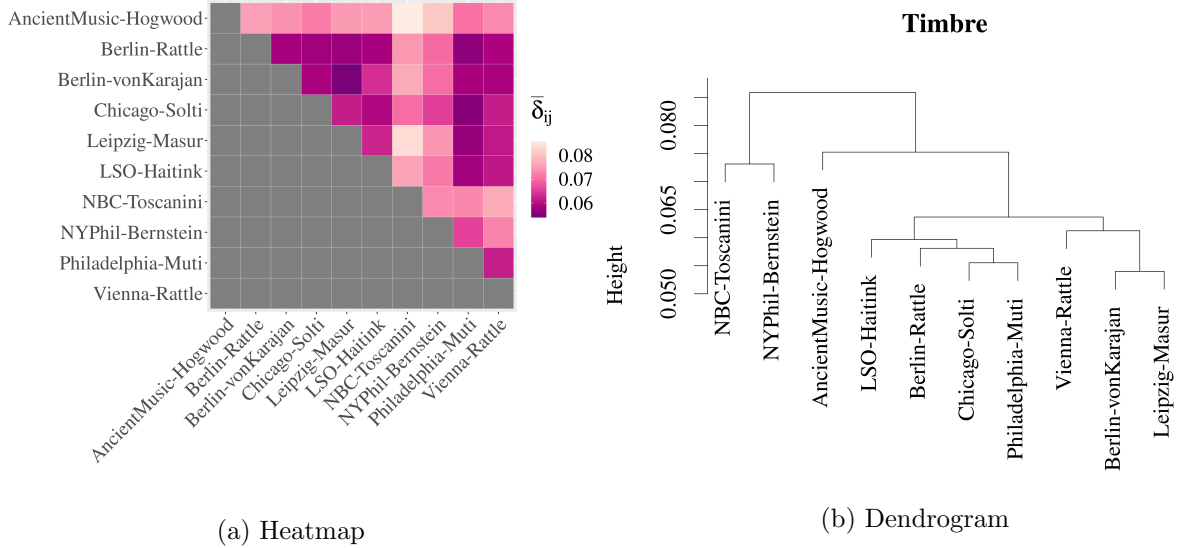


Figure 9: (a) Heatmap of the posterior means of δ_{ij} and (b) dendrogram found via hierarchical agglomerative clustering on the posterior mean of δ_{ij} for the timbre metric. Newer recordings are more similar to each other than older recordings.

tween orchestras across pieces and the τ_p parameters were able to capture variation in the potential for across-orchestra differences. The overall analysis of the posterior means for δ_{ij} , the systematic dissimilarity between orchestras i and j , for the three musical metrics yielded some expected and surprising results. As expected, the recordings by Vienna-Rattle and Berlin-Rattle were found to be very similar across all three musical metrics, but especially tempo, which the conductor has a large influence on. Additionally, the Academy of Ancient Music was confirmed as an outlier in terms of dynamics and timbre, due to their use of period instruments. Surprisingly, we found that NBC and the Academy of Ancient Music were most similar to each other in terms of tempo, and this might be attributed to their adherence to artistic styles from Beethoven’s time.

However, a few other interesting results also emerged. Across all three of the musical metrics, Philadelphia-Muti and Leipzig-Masur were quite similar. This was not an obvious result, as Riccardo Muti and Kurt Masur had different conducting backgrounds and experiences. Additionally, the Philadelphia Orchestra and the Leipzig Gewandhaus Orchestra are both among the most well known American and European orchestras, respectively, with very different histories. Philadelphia is known for the “Philadelphia Sound”, developed under Leopold Stokowski in the early 1900s, while Leipzig has a long and storied history of conductors, including Felix Mendelssohn.

Finally, the evidence for more similarity across tempo, dynamics and timbre in the more recent recordings was not necessarily expected a priori. While some of this is due to changes in recording technology, and the fact that Rattle conducted both the Vienna and Berlin Philharmonics here,

this result suggests that there may be less variation among newer recordings by different orchestras, as compared to older recordings.

It is important to note that in terms of the musical application of interest, tempo was the only metric considered that was independent of the recording technology used for each orchestra’s recordings, and from that perspective, was the most indicative of artistic differences between orchestras. Dynamics and timbre both depend on the specifics of recording technology, and are also related to each other, as louder instruments will have different timbres than softer overall instruments. Additionally, it should be noted that the different orchestras considered performed on different brands and makes of instruments, which also contributed to the differences in dynamics and timbre.

Future extensions to the proposed HMDS model could consider a hierarchical extension to share information across metrics and learn an overall distance for each orchestra pair. Other extensions could include exploring constraints on the parameter space for the X_i vectors to allow for identifiability of these parameters, such as in Bakker and Poole (2013).

Acknowledgements

The authors would like to thank Mike Kris for helpful discussions about the interpretation of results in a musical context.

References

- Marti J. Anderson. A new method for non-parametric multivariate analysis. *Austral Ecology*, 26: 32–46, 2001.
- Andreas Arzt and Stefan Lattner. Audio-to-Score Alignment using Transposition- invariant Features. In *Proceedings of the 19th International Society for Music Information Retrieval Conference*, pages 592–599, Paris, France, September 2018.
- Ryan Bakker and Keith T. Poole. Bayesian Metric Multidimensional Scaling. *Political Analysis*, 21:125–140, 2013.
- Dan Ellis. Chroma feature analysis and synthesis. <https://labrosa.ee.columbia.edu/matlab/chroma-ansyn/>, 2007.
- Duncan K. H. Fong, Wayne S. DeSarbo, Zhe Chen, and Zhuying Xu. A bayesian vector multidimensional scaling procedure incorporating dimension reparameterization with variable selection. *Psychometrika*, 80(4):1043–1065, 2015.

- Andrew Gelman, John B. Carlin, Hal S. Stern, David B. Dunson, Aki Vehtari, and Donald B. Rubin. *Bayesian Data Analysis*. CRC Press, Third Edition edition, 2014.
- Maarten Grachten, Martin Gasser, Andreas Arzt, and Gerhard Widmer. Automatic Alignment of Music Performances with Structural Differences. In *Proceedings of the 14th International Society for Music Information Retrieval Conference*, pages 607–612, Curitiba, Brazil, November 2013.
- International Music Score Library Project. IMSLP: Petrucci Music Library. https://imslp.org/wiki/Category:Beethoven,_Ludwig_van, 2019.
- Julius Kammerl, Neil Birkbeck, Sasi Inguva, Damien Kelly, A. J. Crawford, Hugh Denman, Anil Kokaram, and Caroline Pantofaru. Temporal Synchronization of Multiple Audio Signals. *2014 IEEE International Conference on Acoustics, Speech and Signal Processing (ICASSP)*, 2014.
- Holger Kirchhoff and Alexander Lerch. Evaluation of Features for Audio-to-Audio Alignment. *Journal of New Music Research*, 40(1):27–41, 2011.
- Kunstderfuge.com. Franz Liszt Transcriptions. <http://www.kunstderfuge.com/liszt.htm#Transcriptions>, January 2018.
- Cynthia C. S. Liem and Alan Hanjalic. Comparative Analysis of Orchestral Performance Recordings: An Image-Based Approach. In *Proceedings of the 16th International Society for Music Information Retrieval Conference*, pages 302–308, Málaga, Spain, October 2015.
- L. Lin and Duncan K. H. Fong. Bayesian multidimensional scaling procedure with variable selection. *Computational Statistics & Data Analysis*, 129:1–13, 2019.
- Beth Logan. Mel Frequency Cepstral Coefficients for Music Modeling. In *In International Symposium on Music Information Retrieval*, 2000.
- Brian H. McArdle and Marti J. Anderson. Fitting Multivariate Models to Community Data: A Comment on Distance-Based Redundancy Analysis. *Ecology*, 8(1):290–297, 2001.
- Christopher Minas and Giovanni Montana. Distance-Based Analysis of Variance: Approximate Inference. *Statistical Analysis and Data Mining*, 7(6):450–470, 2014.
- Meinard Müller. *Fundamentals of Music Processing*. Springer, 2015.
- Man-Suk Oh and Adrian E. Raftery. Bayesian Multidimensional Scaling and Choice of Dimension. *Journal of the American Statistical Association*, 96(455):1031–1044, 2001.
- Joonwook Park, Wayne S. DeSarbo, and John Liechty. A Hierarchical Bayesian Multidimensional Scaling Methodology for Accommodating Both Structural and Preference Heterogeneity. *Psychometrika*, 73(3):451–472, 2008.

- Jeroen Peperkamp, Klaus Hildebrandt, and Cynthia C. S. Liem. A Formalization of Relative Local Tempo Variations in Collections of Performances. In *Proceedings of the 18th International Society for Music Information Retrieval Conference*, pages 158–164, Suzhou, China, October 2017.
- Zbigniew W. Raś and Alicja A. Wieczorkowska, editors. *Advances in Music Information Retrieval*, volume 274 of *Studies in Computational Intelligence*. Springer, 2010.
- Maria L. Rizzo and Gabor J. Szekely. DISCO Analysis: A Nonparametric Extension of Analysis of Variance. *The Annals of Applied Statistics*, 4(2):1034–1055, 2010.
- Miguel A. Román, Antonio Pertusa, and Jorge Calvo-Zaragoza. An End-to-end Framework for Audio-to-Score Music Transcription on Monophonic Excerpts. In *Proceedings of the 19th International Society for Music Information Retrieval Conference*, pages 34–41, Paris, France, September 2018.
- Jimena Royo-Letelier, Romain Hennequin, Viet-Anh Tran, and Manuel Moussallam. Disambiguating Music Artists at Scale with Audio Metric Learning. In *Proceedings of the 19th International Society for Music Information Retrieval Conference*, pages 622–629, Paris, France, September 2018.
- Stan Development Team. *Stan Reference Manual*, 2.21 edition, 2019. URL https://mc-stan.org/docs/2_18/reference-manual/effective-sample-size-section.html.
- Stan Development Team. RStan: the R interface to Stan, 2019. URL <http://mc-stan.org/>. R package version 2.19.2.
- Daniel Stoller, Sebastian Ewert, and Simon Dixon. Wave-U-Net: A Multi-Scale Neural Network for End- to-End Audio Source Separation. In *Proceedings of the 19th International Society for Music Information Retrieval Conference*, pages 334–340, Paris, France, September 2018.
- Jerome Sueur. *Sound Analysis and Synthesis with R*. Springer, 2018.
- Jerome Sueur, Thierry Aubin, Caroline Simonis, Laurent Lellouch, Ethan C. Brown, and et. al. Package ‘seewave’: Sound analysis and synthesis. <https://cran.r-project.org/web/packages/seewave/seewave.pdf>, 2018.
- Harvey D. Thornburg, Randal J. Leistikow, and Jonathan Berger. Melody Extraction and Musical Onset Detection from Framewise STFT Peak Data. *IEEE Transactions on Audio, Speech and Language Processing*, 15(4):1257–1272, May 2007.
- W. S. Torgerson. Multidimensional Scaling: I. Theory and Method. *Psychometrika*, 17:401–419, 1952.

Aaron van den Oord, Sander Dieleman, and Benjamin Schrauwen. Deep content-based music recommendation. In C. J. C. Burges, L. Bottou, M. Welling, Z. Ghahramani, and K. Q. Weinberger, editors, *Advances in Neural Information Processing Systems 26*, pages 2643–2651. Curran Associates, Inc., 2013.

Aäron van den Oord, Sander Dieleman, Heiga Zen, Karen Simonyan, Oriol Vinyals, Alex Graves, Nal Kalchbrenner, Andrew W. Senior, and Koray Kavukcuoglu. WaveNet: A Generative Model for Raw Audio. *CoRR*, abs/1609.03499, 2016. URL <http://arxiv.org/abs/1609.03499>.

Igor Vatolkin and Günter Rudolph. Comparison of Audio Features for Recognition of Western and Ethnic Instruments in Polyphonic Mixtures. In *Proceedings of the 19th International Society for Music Information Retrieval Conference*, pages 554–560, Paris, France, September 2018.

Olga A. Vsevolozhskaya, Dmitri V. Zaykin, Mark C. Greenwood, Changshuai Wei, and Qing Lu. Functional Analysis of Variance for Association Studies. *PLOS ONE*, 9(9), 2014.

A Markov Chain Monte Carlo

One possible Markov Chain Monte Carlo algorithm for parameter inference for the HMDS model is outlined in this section. The HMDS model is:

$$y_{ijp} \sim \text{Gamma}\left(\psi, \frac{\psi}{\tau_p \delta_{ij}}\right), \quad j > i, \quad i, j = 1, \dots, N, \quad p = 1, \dots, M.$$

The priors for the HMDS model are:

$$\begin{aligned} \delta_{ij} &\sim \text{Inv-Gamma}(\gamma, (\gamma + 1)\|X_i - X_j\|_2) \\ X_1, \dots, X_N &\stackrel{\text{indep.}}{\sim} N_r(0, \Lambda) \\ \psi &\sim \text{Gamma}(a_1, b_1) \\ \gamma &\sim \text{Gamma}(a_2, b_2) \\ \tau_1, \dots, \tau_M &\stackrel{\text{indep.}}{\sim} \text{Inverse-Gamma}(\alpha, \beta) \end{aligned} \tag{7}$$

The priors for δ_{ij} and τ_p allow for conjugacy and Gibbs sampling for these parameters, while the other parameters require Metropolis-Hastings updates. For ease of notation, let

$$\boldsymbol{\theta} = \left\{ \{\delta_{ij}\}_{j>i}, \{\tau_p\}_{p=1}^M, \{X_i\}_{i=1}^N, \psi, \gamma \right\}.$$

The Gibbs sampling full conditionals and Metropolis-Hastings proposals (up to proportionality)

can be derived as follows:

$$\begin{aligned}
p(\mathbf{Y}) &= \prod_{i=1}^N \prod_{j>i} \prod_{p=1}^M \text{dgamma}\left(y_{ijp} \mid \psi, \frac{\psi}{\tau_p \delta_{ij}}\right) \\
p(\mathbf{\Delta}) &= \prod_{i=1}^N \prod_{j>i} \text{dinv-gam}(\delta_{ij} \mid \gamma, (\gamma + 1) \|X_i - X_j\|_2) \\
p(\mathbf{X}) &= \prod_{i=1}^N \text{dnorm}(X_i \mid 0, \Lambda) \\
p(\boldsymbol{\tau}) &= \prod_{p=1}^M \text{dinv-gam}(\tau_p \mid \alpha, \beta),
\end{aligned}$$

where dgamma, dinv-gam and dnorm are the density functions for the gamma, inverse-gamma and normal distributions, respectively.

$$\begin{aligned}
p(\delta_{ij} \mid \boldsymbol{\theta}_{-\delta_{ij}}) &\propto \text{dinv-gam}(\delta_{ij} \mid \gamma, (\gamma + 1) \|X_i - X_j\|_2) \prod_{p=1}^M \text{dgamma}\left(y_{ijp} \mid \psi, \frac{\psi}{\tau_p \delta_{ij}}\right) \\
&\propto \delta_{ij}^{-(M\psi + \gamma) - 1} \exp\left(-\frac{1}{\delta_{ij}} \left[(\gamma + 1) \|X_i - X_j\|_2 + \psi \sum_{p=1}^M \frac{y_{ijp}}{\tau_p} \right]\right) \\
\implies \delta_{ij} \mid \boldsymbol{\theta}_{-\delta_{ij}} &\sim \text{Inv-Gamma}\left(M\psi + \gamma, (\gamma + 1) \|X_i - X_j\|_2 + \psi \sum_{p=1}^M \frac{y_{ijp}}{\tau_p}\right)
\end{aligned}$$

$$\begin{aligned}
p(\tau_p \mid \boldsymbol{\theta}_{-\tau_p}) &\propto \text{dinv-gam}(\tau_p \mid \alpha, \beta) \prod_{i=1}^N \prod_{j>i} \text{dgamma}\left(y_{ijp} \mid \psi, \frac{\psi}{\tau_p \delta_{ij}}\right) \\
&\propto \left[\prod_{i=1}^N \prod_{j>i} \left(\frac{\psi}{\tau_p \delta_{ij}}\right)^\psi \frac{1}{\Gamma(\psi)} y_{ijp}^{\psi-1} \exp\left(-\frac{y_{ijp} \psi}{\tau_p \delta_{ij}}\right) \right] \tau_p^{-\alpha-1} \exp\left(-\frac{\beta}{\tau_p}\right) \\
&\propto \tau_p^{-(N-1)N\psi/2 - \alpha - 1} \exp\left(-\frac{1}{\tau_p} \left[\beta + \sum_{i=1}^N \sum_{j>i} \frac{y_{ijp} \psi}{\delta_{ij}} \right]\right) \\
\implies \tau_p \mid \boldsymbol{\theta}_{-\tau_p} &\sim \text{Inv-Gamma}\left(\tau_p \mid \alpha + \frac{N(N-1)}{2} \psi, \beta + \psi \sum_{i=1}^N \sum_{j>i} \frac{y_{ijp}}{\delta_{ij}}\right)
\end{aligned}$$

$$\begin{aligned}
p(\psi|\boldsymbol{\theta}_{-\psi}) &\propto \text{dgamma}(\psi|a_1, b_1) \prod_{i=1}^N \prod_{j>i}^M \prod_{p=1}^M \text{dgamma}\left(y_{ijp}|\psi, \frac{\psi}{\tau_p \delta_{ij}}\right) \\
&\propto \psi^{a_1-1} e^{-b_1 \psi} \prod_{i=1}^N \prod_{j>i}^M \prod_{p=1}^M \left(\frac{\psi}{\tau_p \delta_{ij}}\right)^\psi y_{ijp}^{\psi-1} \exp\left(-y_{ijp} \frac{\psi}{\tau_p \delta_{ij}}\right) \\
\implies p(\psi|\boldsymbol{\theta}_{-\psi}) &\propto \left[\frac{\psi^\psi}{\Gamma(\psi)}\right]^{\frac{N(N-1)M}{2}} \left[\prod_{i=1}^N \prod_{j>i}^M \prod_{p=1}^M \left(\frac{y_{ijp}}{\tau_p \delta_{ij}}\right)^\psi \right] \text{dgamma}\left(\psi \middle| a_1, b_1 + \sum_{i=1}^N \sum_{j>i}^M \sum_{p=1}^M \frac{y_{ijp}}{\tau_p \delta_{ij}}\right)
\end{aligned}$$

A Metropolis-Hastings step can again be used to update ψ , where the proposal distribution ensures that $\psi > 0$.

$$\begin{aligned}
p(\gamma|\boldsymbol{\theta}_{-\gamma}) &\propto \text{dgamma}(\gamma|a_2, b_2) \prod_{i=1}^N \prod_{j>i} \text{dinv-gam}(\delta_{ij}|\gamma, (\gamma+1)\|X_i - X_j\|_2) \\
&\propto \gamma^{a_2-1} e^{-b_2 \gamma} \prod_{i=1}^N \prod_{j>i} ((\gamma+1)\|X_i - X_j\|_2)^\gamma \frac{1}{\Gamma(\gamma)} \delta_{ij}^{-\gamma-1} \exp\left(-\frac{(\gamma+1)\|X_i - X_j\|_2}{\delta_{ij}}\right) \\
\implies p(\gamma|\boldsymbol{\theta}_{-\gamma}) &\propto \left(\frac{(\gamma+1)^\gamma}{\Gamma(\gamma)}\right)^{N(N-1)/2} \left[\prod_{i=1}^N \prod_{j>i} \left(\frac{\gamma\|X_i - X_j\|_2}{\delta_{ij}}\right)^\gamma \right] \\
&\quad \times \text{dgamma}\left(\gamma \middle| a_2, b_2 + \sum_{i=1}^N \sum_{j>i} \frac{\|X_i - X_j\|_2}{\delta_{ij}}\right)
\end{aligned}$$

A Metropolis-Hastings step can be used to update γ , where the proposal distribution ensures that $\gamma > 0$.

$$\begin{aligned}
p(X_i|\boldsymbol{\theta}_{-X_i}) &\propto \text{dnorm}(X_i|0, \Lambda) \prod_{j>i} \text{dinv-gam}(\delta_{ij}|\gamma, (\gamma+1)\|X_i - X_j\|_2) \\
&\propto \exp\left(-\frac{1}{2} X_i^T \Lambda^{-1} X_i\right) \prod_{j>i} \frac{((\gamma+1)\|X_i - X_j\|_2)^\gamma}{\Gamma(\gamma)} \delta_{ij}^{-\gamma-1} \exp(-\delta_{ij}(\gamma+1)\|X_i - X_j\|_2) \\
\implies p(X_i|\boldsymbol{\theta}_{-X_i}) &\propto \left[\prod_{j>i} (\|X_i - X_j\|_2)^\gamma \right] \exp\left(-\left[\frac{1}{2} X_i^T \Lambda^{-1} X_i + (\gamma+1) \sum_{j>i} \frac{\|X_i - X_j\|_2}{\delta_{ij}}\right]\right)
\end{aligned}$$

A random-walk Metropolis-Hastings step can be used to update X_i .

B Additional Results

In this section, we present further MCMC approximation, goodness-of-fit checks and parameter results, expanding on the results and analysis presented in Section 4.

B.1 MCMC Approximation and Goodness-of-Fit Checks

We diagnose our MCMC approximation using trace plots and effective sample size diagnostics. Trace plots for a subset of the τ_p values for dynamics (Figure 10a) and timbre (Figure 10b), and for ψ (Figure 12a) and γ (Figure 12b) across all musical metrics appear stationary and to have converged. The δ_{ij} parameters are ordered in terms of their posterior means and the trace plot for every third orchestra pair is plotted in Figure 11 for all three musical metrics. ESS values across parameters and metrics are given in Table 2. The Markov chains appear to be mixing slowly for the δ_{ij} and γ parameters. The ESS values for ψ and some of the X_i 's are larger than 15000 (the number of posterior samples), indicating a negative autocorrelation in the chain for these parameters. Despite the slow mixing indicated by the ESS values, the trace plots across parameters and musical metrics appear stationary.

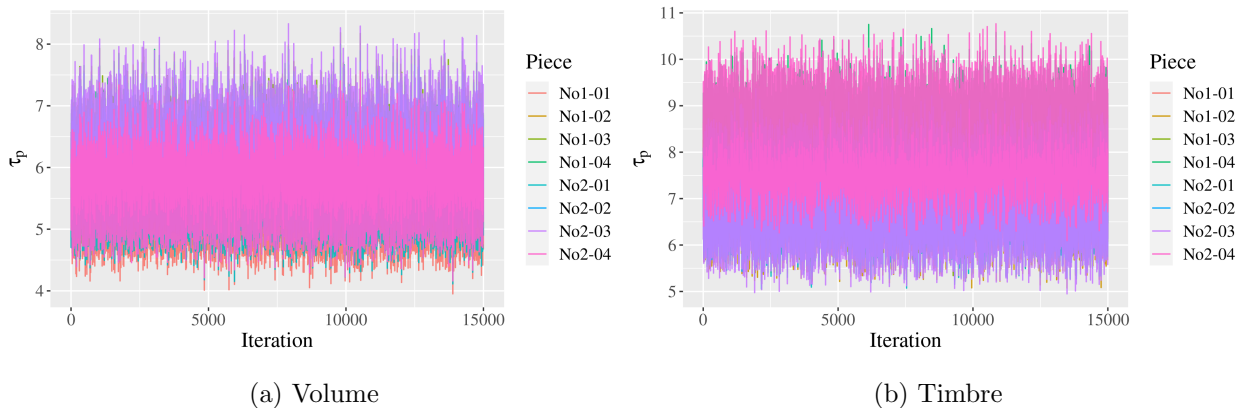


Figure 10: Trace plots for a subset of τ_p values (for Symphonies No. 1 and No. 2, corresponding to $p = 1, \dots, 8$ for the (a) dynamics and (b) timbre metrics.

Table 2: Effective sample sizes for the HMDS parameters. The values for δ_{ij} and X_i are the median ESS values across all orchestra pairs and orchestras, respectively.

	Tempo	Dynamics	SF
δ_{ij}	390	204	266
X_i	12053	7794	12008
ψ	23116	16820	22896
γ	1292	2491	1376

Additionally, we use posterior predictive checks to evaluate the HMDS sampling and hierarchical models, as described in Section 4. Posterior distributions for r_{ijp} for one orchestra pair across all

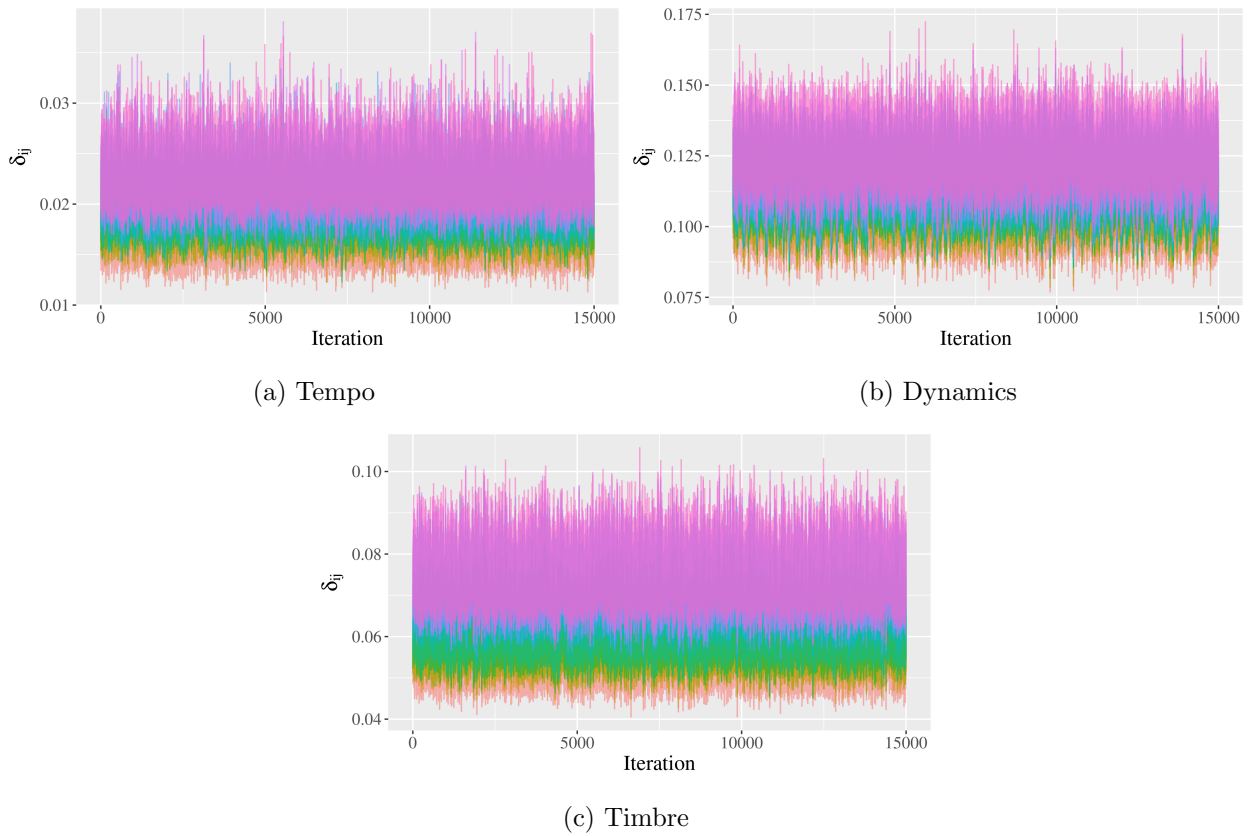


Figure 11: Trace plots for a subset of δ_{ij} pairs for the (a) tempo, (b) dynamics and (c) timbre metrics. All trace plots for δ_{ij} across metrics appear stationary.

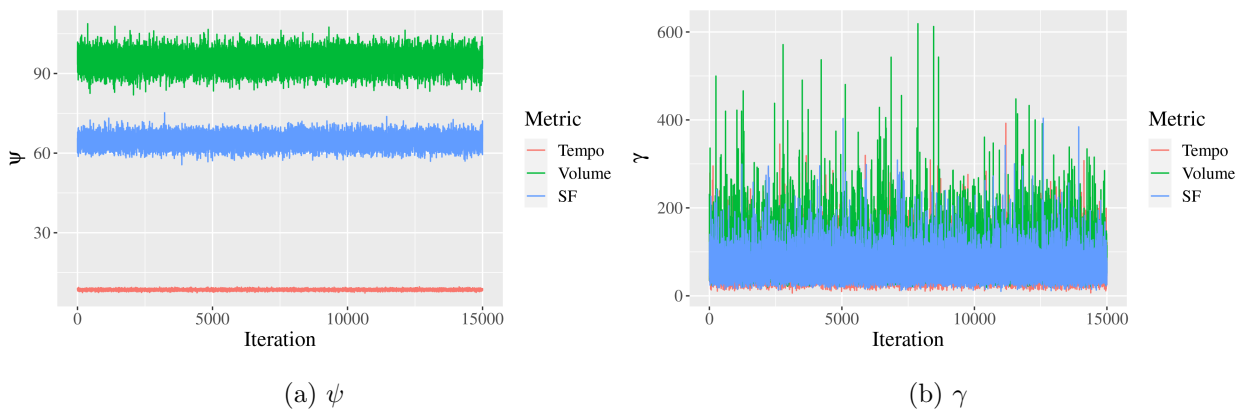


Figure 12: Trace plots for (a) ψ and (b) γ for all three musical metrics. The trace plots again appear stationary.

pieces show good coverage for both dynamics (Figure 13) and timbre (Figure 14) in terms of evaluating the sampling model. Results for the hierarchical model for the dynamics and timbre metrics look identical to the tempo results presented above (Figure 5).

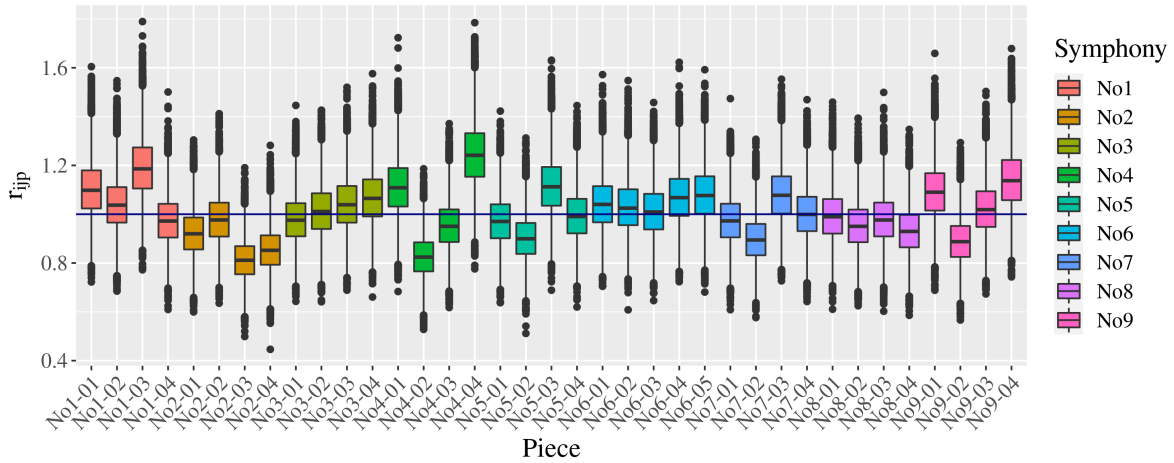


Figure 13: Posterior predictive checks for one orchestra pair (Academy of Ancient Music and Vienna-Rattle) across all pieces for the dynamics metric, $r_{ijp} = \tilde{y}_{ijp}/y_{ijp}$.

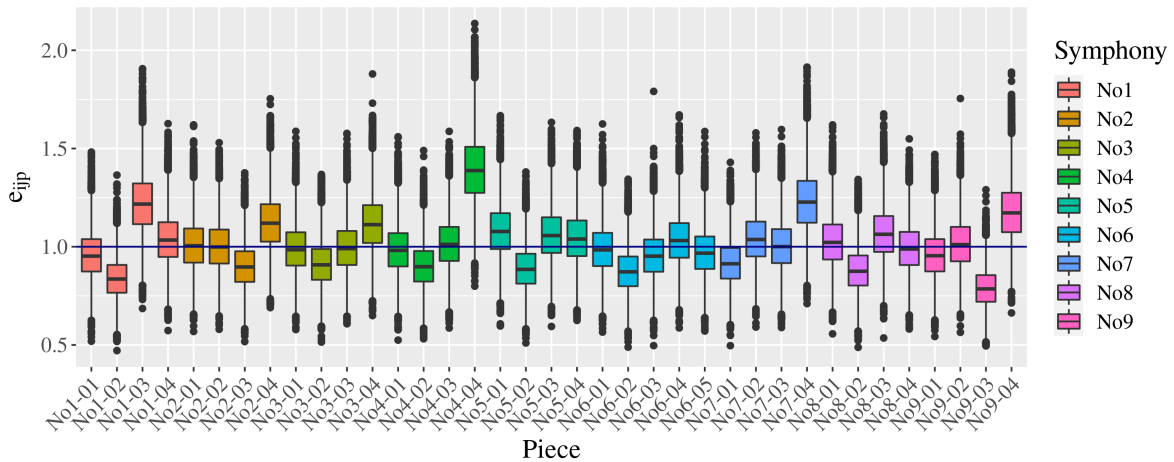


Figure 14: Posterior predictive checks for one orchestra pair (Academy of Ancient Music and Vienna-Rattle) across all pieces for the timbre metric, $r_{ijp} = \tilde{y}_{ijp}/y_{ijp}$.

B.2 Heterogeneous Variation by Piece

The posterior τ_p values are shown for dynamics (Figure 15) and timbre (Figure 16) for all pieces. The results for these metrics also correspond to musical expectation. For example, Symphony No. 6, Movement 4 is the “Storm” movement of the Pastoral symphony. There are several large changes in dynamics (from *pianissimo*, very soft, to *fortissimo*, very loud) across all instruments in the orchestra across this piece, leading to a high potential for variation between different orchestral recordings. Each time there is a marked change in dynamics in the score, each orchestra can interpret the degree to which they change dynamics differently, leading to a high potential for variation. On the other hand, Symphony No. 6, Movement 2 has less extreme volume changes denoted in the score and tends to be quieter overall. This reduction in the number of denoted dynamics changes results in a lower potential for variation, and a lower posterior mean τ_p value than for Symphony No. 6, Movement 4.

In terms of timbre, Symphony No. 9, Movement 4 has the highest posterior mean for τ_p of any piece. This again makes sense, as Symphony No. 9, Movement 4 is the only piece considered that has vocal parts. Singers can vary significantly in the timbre and hence spectral flatness of their voice, especially compared to orchestral instruments, so Symphony No. 9, Movement 4 has a high potential for variation in terms of timbre as compared to the other pieces, which is reflected in the large posterior mean for τ_p for this piece.

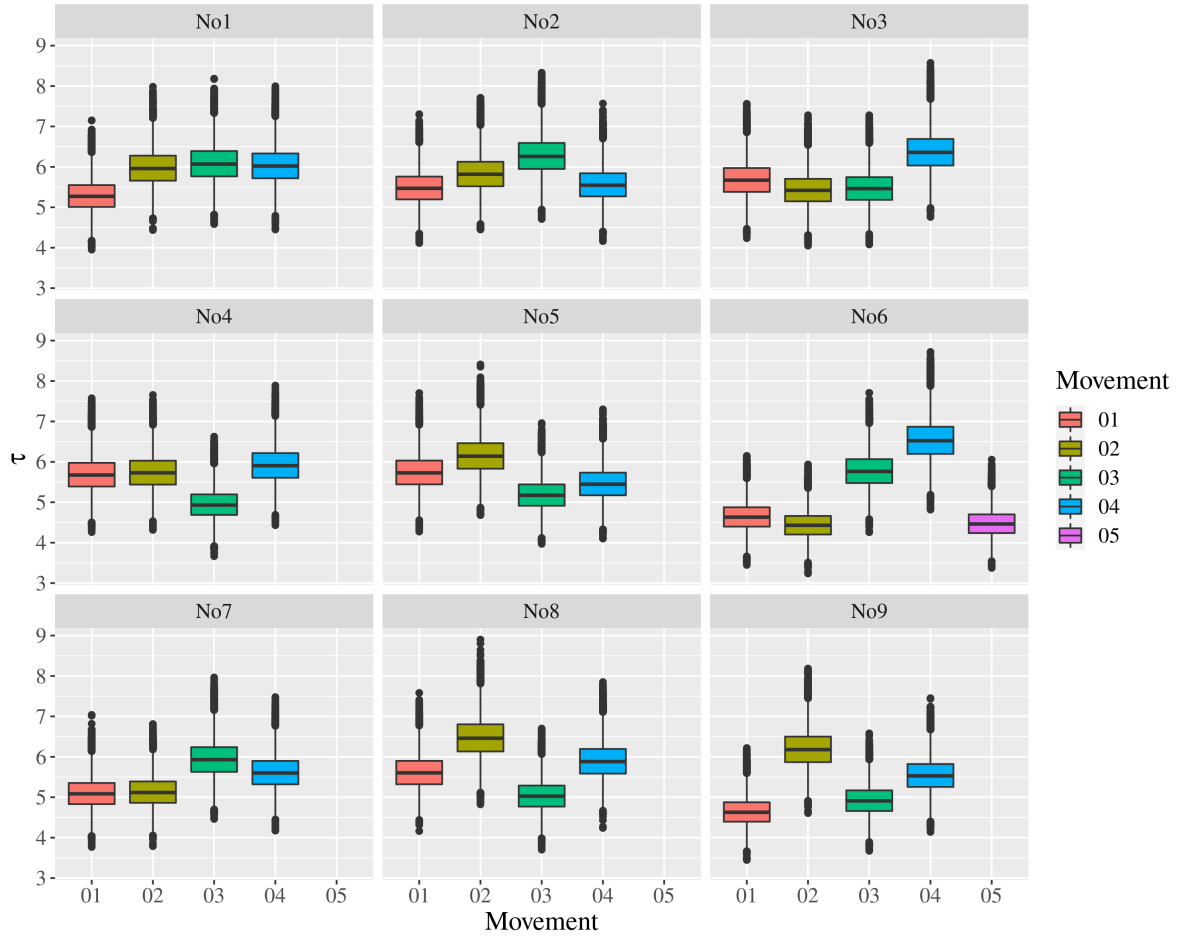


Figure 15: Posterior distributions for the heterogeneous variation parameter, τ_p , for the dynamics metric, by Beethoven symphony. τ_p is able to recover the “potential” for variation by piece.

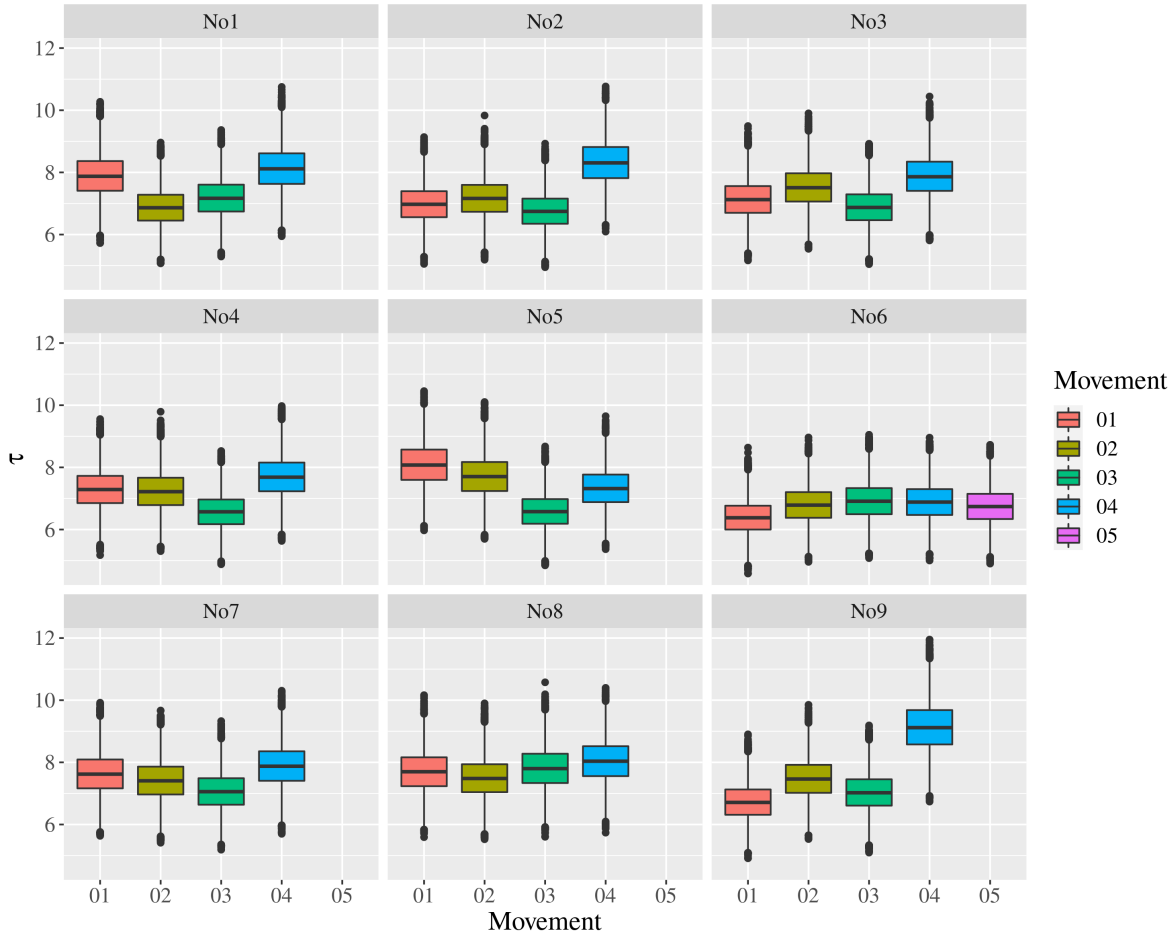


Figure 16: Posterior distributions for the heterogeneous variation parameter, τ_p , for the spectral flatness metric, by Beethoven symphony. τ_p is able to recover the “potential” for variation by piece. For example, the posterior mean of τ_p for No9-04 is much larger than the other pieces, due to the vocal parts in this piece.

B.3 Posterior Distributions for δ_{ij}

While the results in Section 4 focus on the posterior means of parameters, the same general trends hold when the entire posterior distribution for the δ_{ij} parameters is considered. For example, the posterior distribution for δ_{ij} for the Vienna Philharmonic compared to all other orchestras across musical metrics indicates that Vienna tends to be most similar to Berlin-Rattle (Figure 17), especially for the tempo metric. Additionally, the full posterior distributions for δ_{ij} are symmetric across orchestra pairs, which is why the posterior mean is used for analysis in Section 4 .

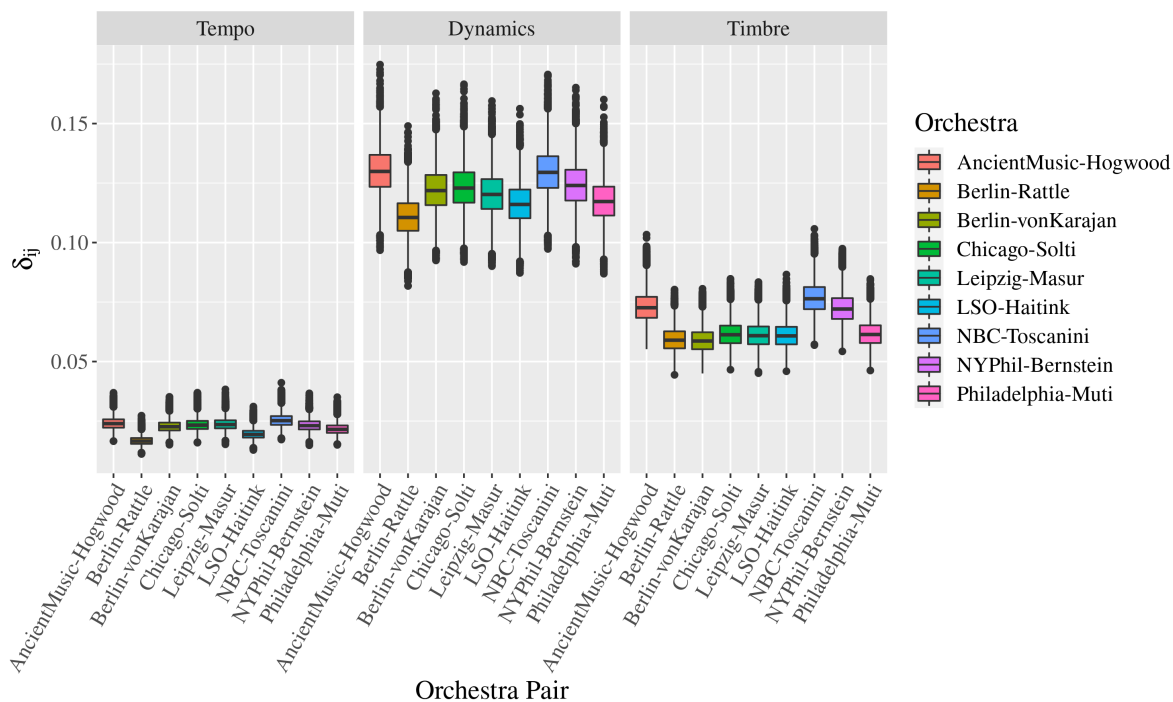


Figure 17: Posterior distributions for the pairwise δ_{ij} values, where $i = \text{Vienna-Rattle}$ for all three metrics. Across metrics, Vienna-Rattle tends to be most similar (smallest δ_{ij}) to Berlin-Rattle.